Brain Struct Funct (2014) 219:433–459
DOI 10.1007/s00429-013-0630-7

REVIEW

Comparison of (stereotactic) parcellations in mouse prefrontal cortex

Henri J. J. M. Van De Werd · Harry B. M. Uylings

Received: 14 February 2013 / Accepted: 24 August 2013 / Published online: 27 September 2013

Abstract This study compares the cytoarchitectonic parcellation of the prefrontal cortex (PFC) in the mouse as presented in publications that are commonly used for identifying brain areas. Agreement was found to be greater for boundaries in the medial PFC than in the lateral PFC and lowest for those in the orbital areas of the PFC. In this review, we explain and illustrate in a selected series of photographs and stereotactic pictures the differences in location and terminology of the different prefrontal cortical areas. The significance of cytoarchitectonic parcellation is discussed.

Keywords Cytoarchitecture · Stereotaxic atlas · Mouse strain · C57BL/6

Abbreviations

ACd	Dorsal anterior cingulate cortex
ACv	Ventral agranular cingulate area
ACvd	Ventral agranular cingulate area, dorsal part
ACvv	Ventral agranular cingulate area, ventral part
AId_1	Dorsal agranular insular area, dorsal part
AId_2	Dorsal agranular insular area, ventral part
AIp	Posterior agranular insular area
cc	Corpus callosum
DI	Dysgranular insular area
DLO	Dorsolateral orbital area
Fr1	Frontal area1
Fr2	Frontal area2
G	Granular cortex
GI	Granular insular area
IG	Indusium griseum
IL	Infralimbic area
LO	Lateral orbital area
MO	Medial orbital area
PFC	Prefrontal cortex
PL	Prelimbic area
PLd	Prelimbic area, dorsal part
PLv	Prelimbic area, ventral part
RSA	Agranular retrosplenial cortex
RSG	Granular retrosplenial cortex
VLO	Ventrolateral orbital area
VLOp	Posterior ventrolateral orbital area
VO	Ventral orbital area

H. J. J. M. Van De Werd · H. B. M. Uylings (✉)
Department of Anatomy and Neuroscience, VU University Medical Center, P.O. Box 7057, 1007 MB Amsterdam, The Netherlands
e-mail: hbm.uylings@vumc.nl

H. J. J. M. Van De Werd
e-mail: werdh@hotmail.nl

Introduction

In our study of the prefrontal cortex (PFC) in mice (Van de Werd et al. 2010), we have defined boundaries of PFC areas on the basis of specified changes in the cytoarchitecture. Moreover, for validation, we have compared the boundaries assessed in the Nissl staining with boundaries visible in a number of histocytochemical stainings. Considerable variations are found in the parcellation of the mouse PFC by different authors. The aim of this study is to review the similarities and differences in the parcellations of the PFC in various atlases and other publications. We will focus on recent atlases, i.e. Hof et al. (2000) and in particular on Franklin and Paxinos (2008), since their atlas is most commonly used. In general, stereotaxic atlases do not explicitly describe cytoarchitectonic features of cortical

boundaries, but they are essential for communication between neuroscientists about a particular brain region on the basis of stereotactic coordinates. To enable better communication about PFC areas we describe the 'Van de Werd et al.' PFC boundaries in a selected series of photographs and stereotactic pictures of the original figures from these atlases. In this way the differences between the parcellations are made directly visible, while our cytoarchitectonic arguments are also made clear. The cytoarchitectonic atlas of Rose (1929) and the studies of Caviness (1975) and Wree et al. (1983) are also included in our review because they give a further illustration of the variations in boundaries of PFC subareas.

Materials and methods

Material

Pairs of 'Nissl' photographs and their corresponding stereotactic drawings, which contain the mouse PFC, were taken from the atlases of Franklin and Paxinos (2008; strain C57BL/6) and Hof et al. (2000; strain C57BL/6). From Rose (1929; strain unspecified) and Cavines (1975; hybrid mice C3H × C57BL/6J) 'Nissl' photographs and from Wree et al. (1983; strain BULB/c) pairs of 'Nissl' photographs and the accompanying Grey Level Index (GLI) pictures were analyzed from the frontal region. The selected photographs and stereotactic schemes represent coronal sections from the anterior part of the PFC to the beginning of the retrosplenial region. In general, cytoarchitectonic delineation characteristics are sufficiently visible in these original Nissl photographs to allow a comparison of the original parcellations with our parcellation (Van de Werd et al. 2010; strain C57BL/6).

The original Nissl-photographs and stereotactic drawings have been transferred into Corel Draw 12 to insert the cortical boundaries of the prefrontal areas based upon our criteria. After the completion of these drawings, the Corel Draw files were converted into PDF files and TIFF files to provide the figures for this paper.

Cytoarchitectonic criteria and nomenclature

Our approach in cytoarchitectonic parcellation is the characterization of the cytoarchitectonic features of the boundaries between cortical areas (Van Eden and Uylings 1985; Uylings and Van Eden 1990; Van de Werd et al. 2010; Uylings et al. 2010). A condition for the characterization of boundaries is that their description can be applied for reproducible delineation by other students. We prefer such an approach to the mere characterization of the areas as a whole, which is the general practice of cytoarchitectonic descriptions. The criteria used in this study have already been published in previous papers (Van de Werd and Uylings 2008; Van de Werd et al. 2010) and they are based on the following criteria: (a) granularity of layer IV, (b) presence and direction of curvilinear columns/rows of cell somata through the layers, (c) visibility of separate (sub)layers, (d) cell density and relative soma sizes in the different cortical layers, (e) dispersion or clustering of somata in layers, and (f) absolute and relative thickness of cortical layers and (g) relative position of cortical layers. These characteristics have been summarized in Appendix 1. The stereotaxic levels are presented by the distance to the Bregma as indicated in the atlas of origin, i.e., the Franklin and Paxinos atlas (2008) for Figs. 1, 2, 3, 4, 5, 6, 7, 8, 9, 10, and the Hof et al. atlas (2000) for Figs. 11, 12, 13, 14, 15, 16, 17, 18, 19.

Results

In the descriptions we have used bold letters to indicate the 'Van de Werd et al' nomenclature, and italics for the nomenclature of the authors of the atlases. In the photographs we have used regular letters to indicate our abbreviations. The stereotaxic atlas of Franklin and Paxinos (2008) offers access to high resolution plates. The atlas of Hof et al. (2000) offers 300 DPI resolution plates on CD-ROMs.

Comparison with the parcellation by Franklin and Paxinos (2008)

General remarks

On the lateral side of the frontal lobe, in contrast with the atlas of Franklin and Paxinos (2008), we have chosen to draw the boundaries up to the white matter. As a consequence the claustrum is included in our parcellation of the lateral PFC although, strictly speaking, it is not part of the PFC.

Frontal pole

Bregma 2.80 mm (Fig. 1): The lateral boundary of the frontal area 2, **Fr2**, is approximately equal to the boundary between the *prelimbic area* (*PrL*) and the *frontal association cortex* (*FrA*). **Fr2** is equal to the dorsolateral part of *PrL*, in contrast to Fig. 2. *PrL* corresponds to the very high activity of acetylcholinesterase in layer III, rather than to the characteristics visible in the Nissl stain. At this level *PrL* encompasses, in addition to area **Fr2**, the dorsal anterior cingulate area (**ACd**) and the dorsal part of the prelimbic area (**PLd**); see Appendix 1 for differentiating

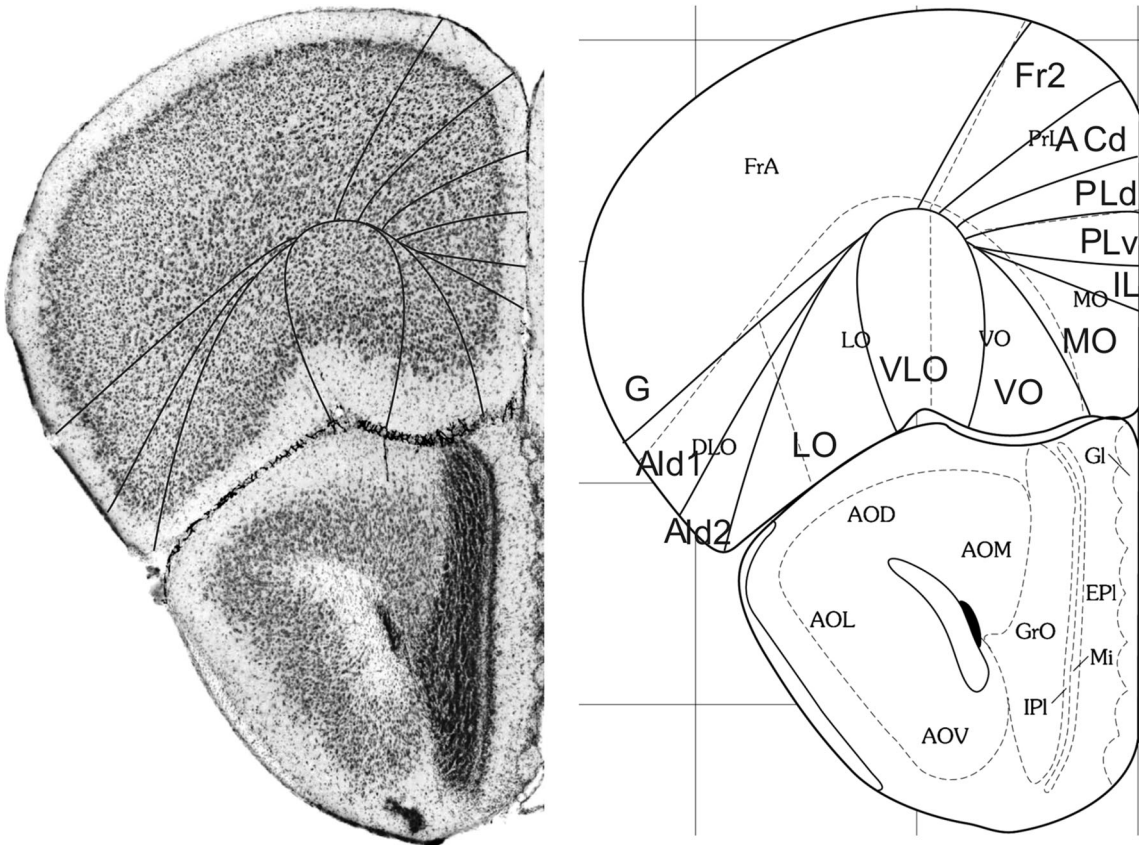

Fig. 1 Implementation of 'Van de Werd et al. (2010)' boundaries at Bregma 2.80 mm (adapted from Franklin and Paxinos 2008)

cytoarchitectonic characteristics. In the ventral part of the medial PFC, which encompasses the ventral prelimbic area (**PLv**), the infralimbic area (**IL**) and the medial orbital area (**MO**), the general density of cell-packing is higher than in the dorsal part of the medial PFC. These three areas offer a more detailed parcellation of the ventral part of the medial PFC than shown in the atlas, in which the whole ventral part of the medial PFC consists of only the *medial orbital area* (*MO*). On the lateral side of the frontal lobe in Franklin and Paxinos (2008), the dorsolateral orbital area *DLO* is specified as a more or less quadrangular field along the ventro-lateral side of the frontal lobe (Figs. 1, 2). In the parcellation of Van de Werd et al. (2010), only the dorsal agranular insular areas **AId1** and **AId2** are present as areas of the lateral PFC. In the mouse, Van de Werd et al. (2010) did not find the characteristic cytoarchitecture of area **DLO** as defined in the rat (Van de Werd and Uylings, 2008). The cytoarchitecture of **AId1** and **AId2** in Fig. 1 is not different from the cytoarchitecture of these areas more posteriorly. At this level, **AId1** is located ventrally to the granular cortex, **G**. The parcellation on the ventral/orbital side of the frontal lobe will be discussed in the evaluation of the next figure, Fig. 2.

Bregma 2.58 mm (Fig. 2): The characteristics of the boundaries in the medial PFC are more clearly visible than they were in Fig. 1. At this level **Fr2** is no longer included in *PrL*, but is now located in *FrA*, due to the change of the dorsal border of *PrL* into a more medial position at this level. *PrL*, therefore, here includes a large part of **ACd** and **PLd**. On the lateral side of the frontal lobe, the dysgranular insular area (**DI**) becomes visible between the ventral end of the band of layer IV granular cells that characterizes the granular cortex and the dorsal agranular insular area, dorsal part, (**AId1**). In the atlas a *DI* area is only specified more caudally (see Figs. 5, 6, 7, 8, 9, 10). In Fig. 2 **DI** is located in *FrA*. Here the curvilinear arrangement of cells in the dorsal agranular insular areas **AId1** and **AId2** is better visible than in the previous Figure, as is the difference in the packing density of the cellular columns in these areas. On the ventral/orbital side of the frontal lobe, Van de Werd et al. (2010) distinguish the areas **VO**, **VLO** and **LO** (see Appendix 1), whereas no **VLO** is defined in the atlas, so that *ventral orbital area* (*VO*) encompasses areas **VO** and a large part of **VLO**, which are cytoarchitectonically different (see Appendix 1).

Frontal lobe anterior to the forceps minor

Bregma 2.34 mm (Fig. 3): At this level area **Fr2** corresponds to the medial part of the *secondary motor area* (*M2*)

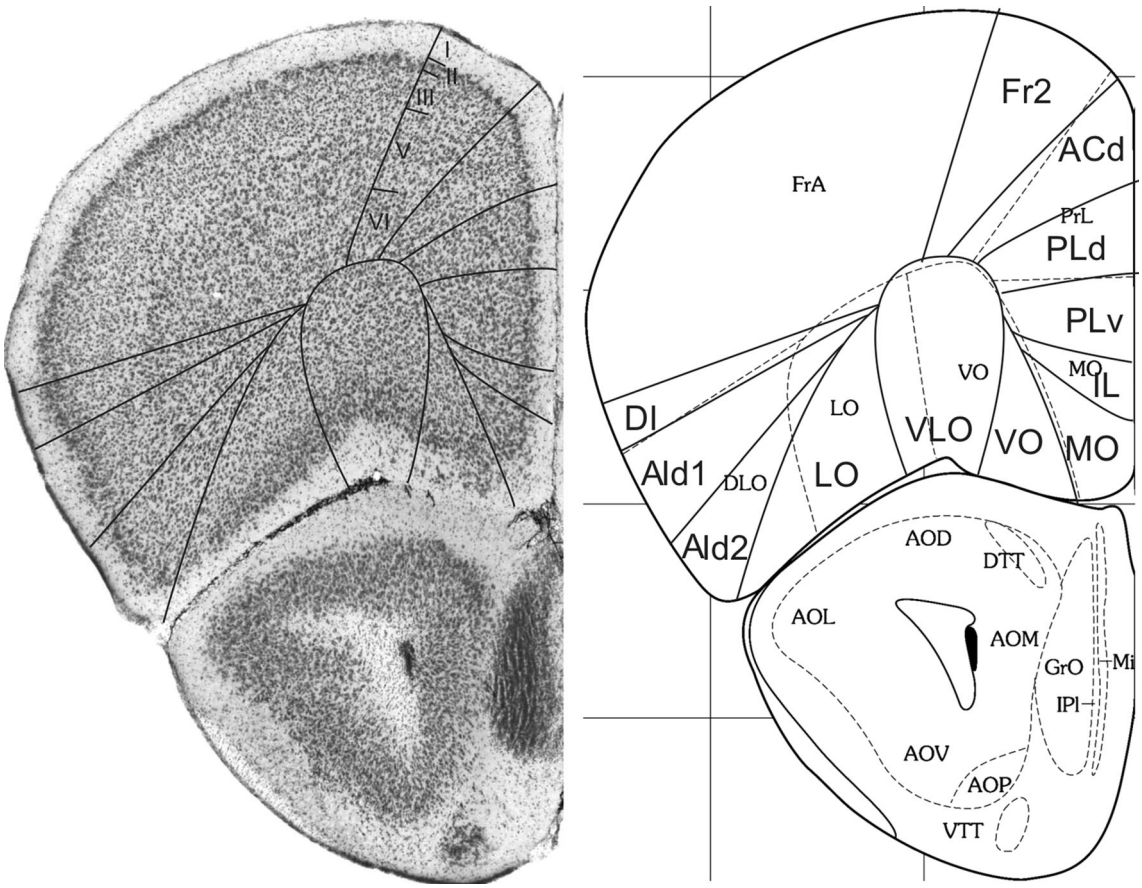

Fig. 2 Implementation of 'Van de Werd et al. (2010)' boundaries at Bregma 2.58 mm (adapted from Franklin and Paxinos 2008)

and this correspondence remains visible more caudally. The *cingulate area 1, Cg1*, is now indicated in the atlas, which is approximately in the same location as **ACd**. The dorsal boundary of *PrL* has moved a little more into ventral direction. *PrL* now encompasses **PLd** and a dorsal part of **PLv**.

The location of area **VO**, which is different from the *ventral orbital area* (*VO*), now contacts the retrobulbar region, i.e. the region behind the olfactory bulb encompassing the anterior olfactory nucleus. **VO**, **MO**, **IL** and the ventral part of **PLv**, are located in *MO*. At this level, **VLO** is largely in agreement with *VO*.

In the lateral PFC, the atlas defines a *ventral agranular insular area, AIV*, at this level, which roughly corresponds to **AId2**. In Van Eden and Uylings (1985), Ray and Price (1992), and Van de Werd and Uylings (2008) **AIV** in the rat is defined as an area in the dorsal bank of the rhinal fissure. In the mouse, however, the **AIv** characteristics are not clearly found, so that they are not specified in the mouse sections. The *dorsal agranular insular area, AID,* is somewhat larger than **AId1**.

Bregma 2.10 mm (Fig. 4): The areas **ACd** and *Cg1* are nearly equal in size and position. *PrL* is nearly equal to **PLd** plus **PLv** of **PL**, and **AId1** and **AId2** are approximately equal to the areas *AID* and *AIV*, respectively. The cortical layers in **VLOp** are more homogeneous than in area **VLO** in the anterior (Figs. 1, 2, 3). **VLOp** is approximately equal to area *VO*.

Frontal lobe anterior to the genu of the corpus callosum

Bregma 1.94 mm (Fig. 5): The areas of the medial PFC are well distinguishable by the cytoarchitectonic differences in layer II, the cellular columns in the areas **Fr2** and **ACd**, and the arrangement of cells in the layer VI in rows, parallel to the cortical surface in the areas **PLd**, **PLv**, **IL** and **MO** (see Appendix 1). *PrL* is approximately in the same location as **PLd** and **PLv**. On the lateral side of the frontal lobe, the prefrontal cortical layers can be followed as far as the piriform cortex. Cytoarchitectonic features of **LO** are at this level not distinguishable.

Bregma 1.70 mm (Fig. 6): The major change with the previous figure is the absence of area **AId2** and the presence of the posterior agranular insular area (**AIp**). The area **AIp** is distinguished by the lower cell density in layer

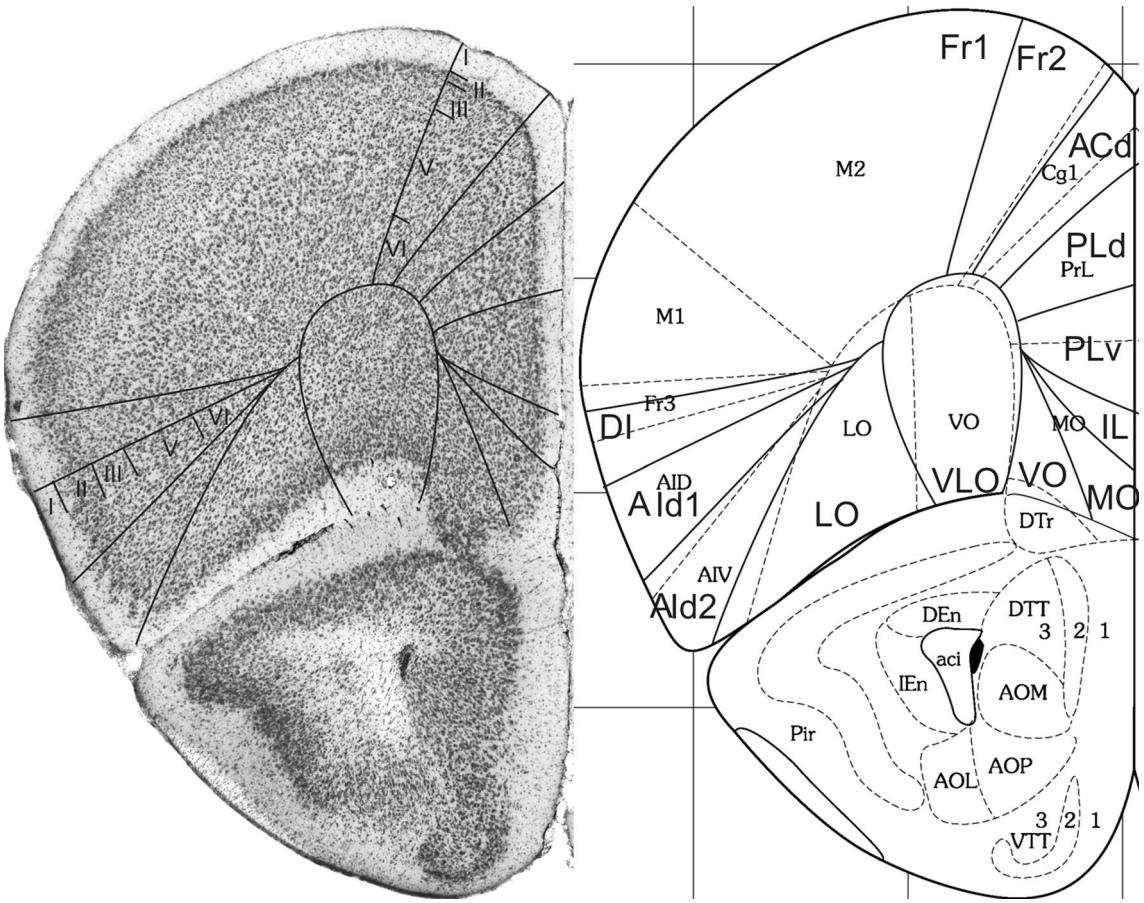

Fig. 3 Implementation of 'Van de Werd et al. (2010)' boundaries at Bregma 2.34 mm (adapted from Franklin and Paxinos 2008. *Fr1* frontal area1

III and the small cells of layer V in comparison with **AId1** (see Appendix 1). At this level, the atlas maintains the *AID* and *AIV* designations. In the medial PFC, the ventral border of **PLv** is more ventral than the ventral border of *PrL*. The ventral border of **MO** is roughly the ventral boundary of *IL* as it is in Fig. 5.

Bregma 1.42 mm (Fig. 7): Within area *M2*, boundary **Fr2/Fr1** is easily defined by the typical characteristic differences in layer II, the position of layer V in relation to the pial surface, and the difference in the cellular columns in layers V and VI on both sides of the boundary. Area **ACd** is roughly *Cg1*. Given the cytoarchitectonic features described in Appendix 1, the **PLd/PLv** boundary is located within *Cg2*. The *Cg2/IL* boundary corresponds with the **PLv/IL** boundary. At this level in the atlas *IL* has a greater extension in ventral direction. In the medial PFC we still define the areas **PLd**, **PLv** and **IL** because the features of these areas are more in line with the cytoarchitectonic criteria for these areas than with the criteria for ventral anterior cingulate areas (see Appendix 1). The differences in the lateral prefrontal areas are quite similar to those described in Fig. 6.

Frontal lobe PFC dorsal to the corpus callosum

Bregma 1.18 mm (Fig. 8): Boundary **Fr2/Fr1** is defined within *M2*, as in nearly all previous figures. The characteristics of boundaries **Fr2/Fr1** and **Fr2/ACd** are all present, and typical. The boundary **Fr2/ACd** is similar to the *M2/Cg1* boundary. The characteristics of boundary **ACd/ACvd** differ from the characteristics of boundary **ACd/PLd** mainly in as far as in **ACvd**, layer III is wider and contains less densely packed cells than in **PLd**. The boundary **ACd/ACvd** is mainly characterized by the difference in layer II, which is narrow in **ACd** and shows densely packed cells at the boundary with layer I, but in **ACvd** this layer is slightly broader and contains densely packed cells (see also Appendix 1 for other features). This boundary is located within *Cg1*. Boundary **ACvd/ACvv** is characterized on the basis of layers II, III, V and VI (see Appendix 1). On the basis of their typical characteristics, boundary **ACvd/ACvv** is in the dorsal half of *Cg2*. The distinction of **AIp** instead of **AId2** or *AIV* in this figure is based on the well separated (sub)layers and the smaller cells of layer V in **AIp** as compared with **AId1** or *AID*.

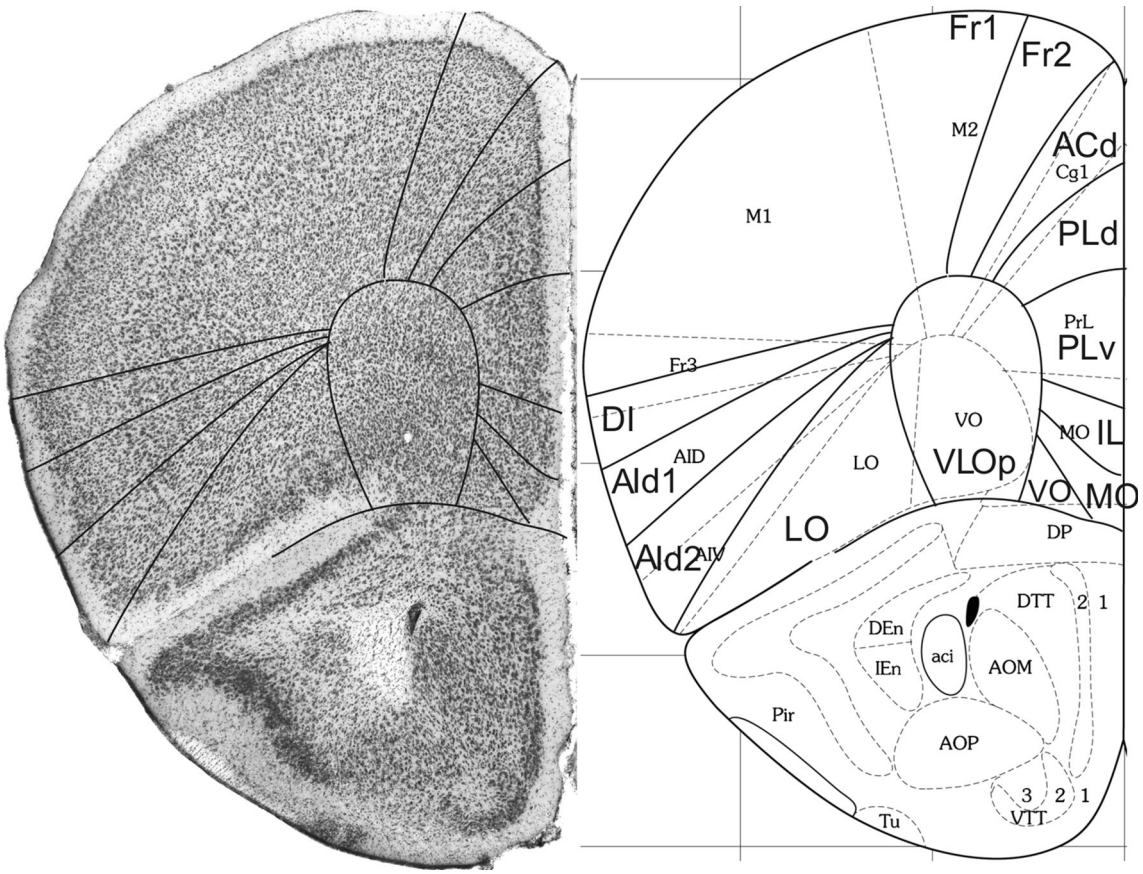

Fig. 4 Implementation of 'Van de Werd et al. (2010)' boundaries at Bregma 2.10 mm (adapted from Franklin and Paxinos 2008)

Bregma 0.74 mm (Fig. 9): Boundary **Fr2/Fr1**, located in area *M2*, is mainly defined on the basis of the characteristics of layer V and the cellular columns in layers V and VI. All other boundaries are clearly distinguishable with the characteristics described for the previous figure. At this level, *Cg1* is approximately in the same location as **ACd**. Boundary **ACvd/ACvv** is in the dorsal half of *Cg2*. No **AId1**, as defined in Appendix 1, is detectable at this level.

Bregma −0.46 mm (Fig. 10): In the medial PFC, the figure shows denser packing of cells in the **ACv** subareas **ACvd** and **ACvv** than in the areas **Fr2** and **ACd**. The figure is also illustrative of the absence of cellular columns in **ACvd** and **ACvv** and their presence in the dorsal areas **Fr2** and **ACd**. In both **ACvd** and **ACvv** the cells of layer VI are arranged in rows, parallel to the cortical surface, but not in **Fr2** and **ACd**. These four clearly distinguishable areas demonstrate that a more detailed parcellation of the medial PFC is possible than is shown in the atlas. Here, **ACd** is smaller than *Cg1*. At this level, the atlas indicates the presence of *posterior agranular insular area, AIP* in the lateral frontal cortex. The distinction and location of **DI** and **AIp** are roughly similar to *GI*, and *DI* and *AIP* in the atlas.

Bregma −0.94 mm: The retrosplenial region which includes the agranular retrosplenial area (**RSA**) and the granular retrosplenial area (**RSG**) is immediately caudal to the PFC region. The retrosplenial region is well identifiable by the very typical narrow band of densely packed granular cells in layer II of area **RSG**. **RSA** and **RSG** correspond with *RSD* and *RSGc*, respectively. This means that the boundary with *M2* is here identical.

Summary

The similarities between the parcellation in the plates of the atlas and our parcellation are found between the areas **ACd** and *Cg1* from Bregma 2.34 mm (Fig. 3) until −0.46 mm (with the exception of Figs. 8, 10), between the combined areas **PLd** and **PLv**, and *PrL* (except for the most anterior sections where *PrL* is positioned dorsomedially), and in the position of area **Fr2** as medial part of area *M2*. **ACd**, however, starts more anteriorly in our parcellation than area *Cg1*. Area *PrL* is replaced by *Cg2* more rostrally (Fig. 7) than the combined areas **PLd** and **PLv** by the combined areas **ACvd** and **ACvv** (Fig. 8). The area **LO** is, in general, nearly similar to area *LO* (Figs. 3,

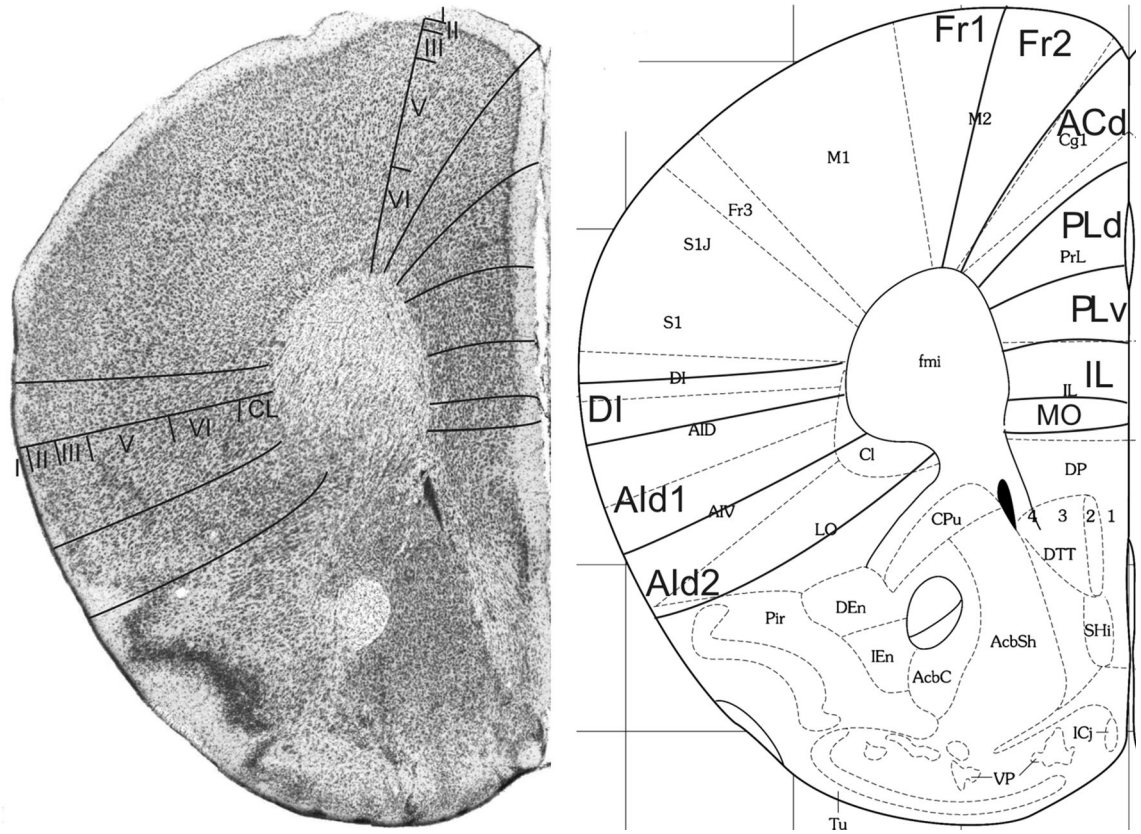

Fig. 5 Implementation of 'Van de Werd et al. (2010)' boundaries at Bregma 1.94 mm (adapted from Franklin and Paxinos 2008)

4), except for the most anterior sections, where the atlas also distinguishes *DLO* (Figs. 1, 2).

The main differences between the atlas and our parcellation concern the size of the medial orbital area (*MO* is much larger than **MO**) (Figs. 1, 2, 3, 4), the presence of *DLO* in the atlas and the absence of this area in our parcellation. In our parcellation, the infralimbic area **IL** starts more anteriorly (Fig. 1) than area *IL* in the atlas (Fig. 5). The cross-sectional size of area *IL* is much larger than the one of **IL** (Figs. 5, 6, 7). In the atlas, the presence of *MO* in anterior sections is replaced by the presence of *IL* in posterior sections. In our parcellation, **MO** and **IL** are both present in many sections. **VO** is sometimes located in *VO* (Figs. 1, 2) and sometimes in *MO* (Figs. 3, 4). **VLO** is not defined in the atlas.

Area **AIp** starts anterior to area *AIP* by first replacing area **AId2** (Fig. 6) and then area **AId1** also (Fig. 9). No **AIv** area is detected in the mouse, while an *AIV* is specified in the atlas (Figs. 3, 4, 5, 6, 7, 8, 9). In the atlas, *AIP* replaces the combined areas *AID* and *AIV*.

In the areas **PL** and **ACv** we distinguish a dorsal and ventral part, **PLd** and **PLv**, and, **ACvd** and **ACvv**, respectively. In the atlas, such a distinction is not made in the areas *PrL* and *Cg2*, respectively.

Comparison with the parcellation by Hof et al. (2000)

In their atlas, Hof et al. have indicated the boundaries between cytoarchitectonic areas by means of arrows positioned at the pial surface. In the original 'image'-files of Nissl sections in Hof et al., curvilinear boundaries have been assessed according to the 'Van de Werd et al.' parcellation. Where cytoarchitectonic characteristics were insufficient, e.g. by artifacts, we had to extrapolate from characteristics visible in the contralateral side, or from an anterior or posterior section.

Frontal pole

In Fig. 11, at *Bregma 2.50 mm*, the characteristics of the PFC boundaries are difficult to distinguish. They could only be reliably identified together with extrapolation from the contralateral hemisphere and from the section shown in Fig. 12. Some features are recognized without extrapolation. For example, on the medial side, the widening of layer II in ventral direction is clearly visible, as is the higher concentration of cells on the boundary between layers I and II in the dorsal half of the medial PFC. In the areas delineated by us as **VO**, **VLO**, **LO** on the ventral side, and

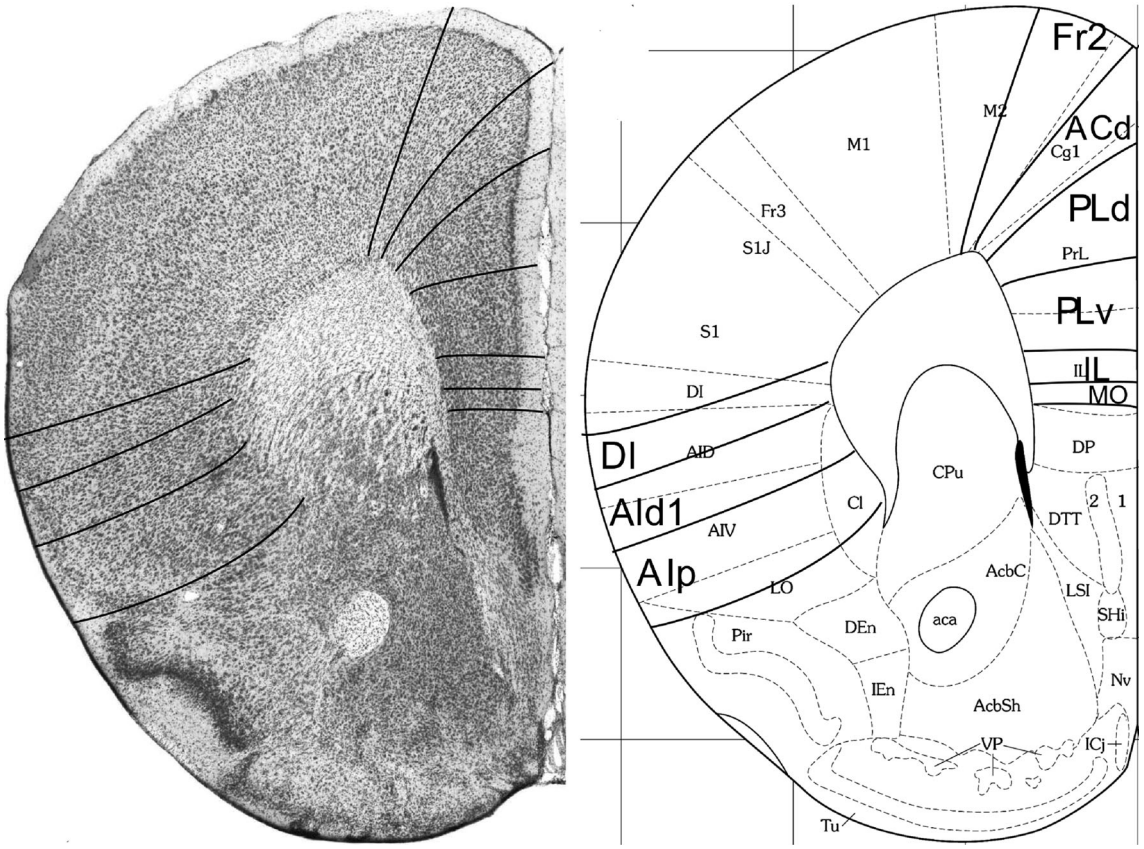

Fig. 6 Implementation of 'Van de Werd et al. (2010)' boundaries at Bregma 1.70 mm (adapted from Franklin and Paxinos 2008)

as **AId1** and **AId2** on the lateral side, mutual differences in the cytoarchitecture are visible that support our parcellation. In the PFC, only four areas are recognized in the atlas of which especially the *orbital cortex, lateral part* (*ORBl*) shows at least three different cytoarchitectonic structures.

Frontal lobe anterior to the forceps minor

In Fig. 12 (*Bregma 2.40 mm*) the areas of the PFC are much easier to distinguish than in the previous figure. Thus, the smooth aspect of the border between layer I and layer II in **Fr2** and the irregular concentration of cells of layer II at the boundary with layer I in **ACd** is now visible. At this level, **ACd** becomes comparable to *ACd.* The dorsal and ventral parts of **PL** are distinguishable by the characteristic features in layer II. The area **IL** is estimated between the wide layer II of **PLv** and the wide layer II with densely packed and evenly dispersed cells of **MO**. The ventral boundaries of **Fr2**, **ACd**, **PLd** and **IL**, and the lateral boundaries of **MO** and **AId2** correspond with boundaries in the atlas. The structure of **VO** is quite different from the one in the adjacent areas **MO** and **VLO**. What is remarkable and not easy to explain is that in the atlas the area *ORBl* in Fig. 12 is localized in the medial half of the ventral side of the frontal lobe, whereas in Fig. 11 this area occupies the lateral half of the ventral side of the frontal lobe and the ventral part of the lateral cortex. Architectonically, the *dorsal agranular insular area, AId*, in Fig. 12 is not different from area *ORBl* in Fig. 11.

In Fig. 13 at *Bregma 2.00 mm*, area *ORBl* is localized again in the lateral half of the ventral PFC. The area **IL** is now better recognizable as a homogeneous area. The difference in the aspect of layer II and the different packing of cellular columns in the areas **AId1** and **AId2** is decisive for the recognition of these areas. For the assessment of the boundary **VLO/LO**, the cellular columns in the layers II and III in area **VLO** and the clustering of cells in layer II of **LO** are decisive. At this level, the ventral boundaries of **Fr2**, **ACd**, and **IL**, the lateral boundaries of **MO** and **LO**, and the dorsal boundary of **AId1** correspond with boundaries in the atlas.

Frontal lobe anterior to the genu of the corpus callosum

At *Bregma 1.60 mm* (Fig. 14), in the medial PFC cells are more densely packed in the ventral areas **PLv**, **IL** and **MO** than in the dorsal areas **Fr2**, **ACd** and **PLd**. The characteristics of the medial PFC areas are all clearly visible. In our parcellation, more areas are recognized than in the

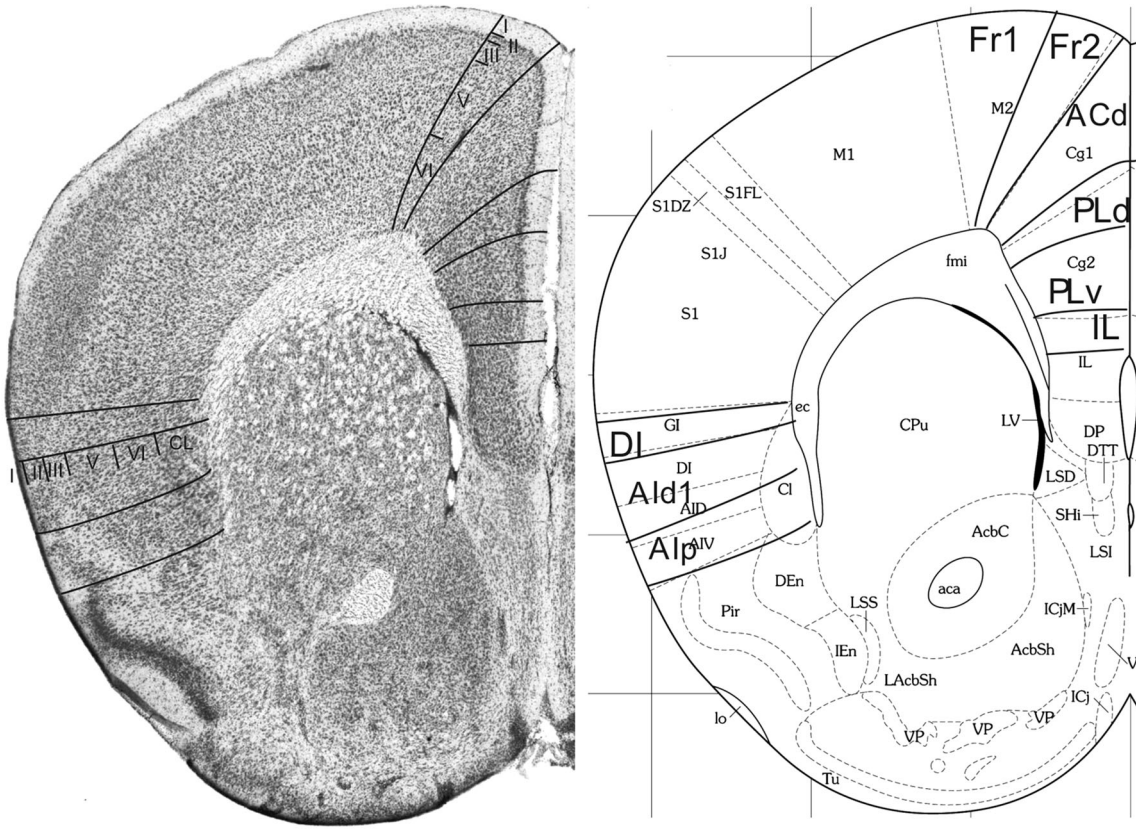

Fig. 7 Implementation of 'Van de Werd et al. (2010)' boundaries at Bregma 1.42 mm (adapted from Franklin and Paxinos 2008)

atlas. The ventral boundaries of **ACd** and **MO** correspond with atlas borders. On the lateral side, the areas **DI**, **AId1** and posterior agranular insular area (**AIp**) are detected. The area **AId1** is distinguished from **DI** by the cellular columns that are visible in **AId1**, not in **DI**. Identification of **DI** and **AId1** is hampered by an artifact in the deeper cortical layers. The dorsal boundary of **DI** is characterized by the end of the layer IV granular band specified by interrupted lines in Fig. 14. The area **AIp** is mainly characterized by the cells in layer V which are smaller than in layer V of **AId1**, and the lower cell density in layer III in **AIp** (see Appendix 1 for other characteristics).

At *Bregma 1.40 mm* (Fig. 15), all characteristics of the boundaries, described in Appendix 1, are distinguishable in the medial PFC. Area **Fr2** becomes comparable with *MOs.* **PLd** and **PLv** together are approximately in the same position as *PL,* and **IL** and **MO** as *IL.* In the lateral PFC, boundaries **DI/AId1** and **AId1/AIp** are more or less in accordance with the original boundaries in the atlas between the *gustatory cortex* and the *agranular insular cortex, dorsal part* (*GU/AId*) and between *AId* and the *agranular insular cortex, ventral part* (*AId/AIv*), respectively. The ventral boundary of **AIp** equals the ventral boundary of *AIv*.

Bregma 1.30 mm (Fig. 16): In the medial PFC, the medial boundary of **Fr2**, the ventral boundaries of **ACd**, **PLd** and **IL** coincide with boundaries in the atlas. On the lateral side of the frontal lobe the areas **DI**, **AId1** and **AIp** approximately correspond with *GU, AId* and *AIv*, respectively.

Frontal lobe PFC dorsal to the corpus callosum

Bregma 1.10 mm (Fig. 17): At this level, **Fr2** is comparable with the medial half of *MOs* and **ACd** corresponds with *ACd.* The subdivision of **ACv** into a dorsal (**ACvd**) and a ventral (**ACvv**) part is supported by the different cytoarchitecture that is visible in these subareas in this Fig. 17. **ACvd** and **ACvv** together coincide with *ACv*. On the lateral side of the frontal lobe, **DI** is more or less comparable to *AId*. At this level, we only distinguish **AIp** (see Appendix 1 for defining characteristics). **AIp** is approximately in the same location as *AIv*.

Bregma 0.70 mm (Fig. 18): At this level, the atlas now also identifies the *posterior agranular insular area, AIp* in the lateral PFC, which corresponds with **AIp**. The similarities and differences between the atlas and our distinctions in the medial PFC are as in Fig. 17.

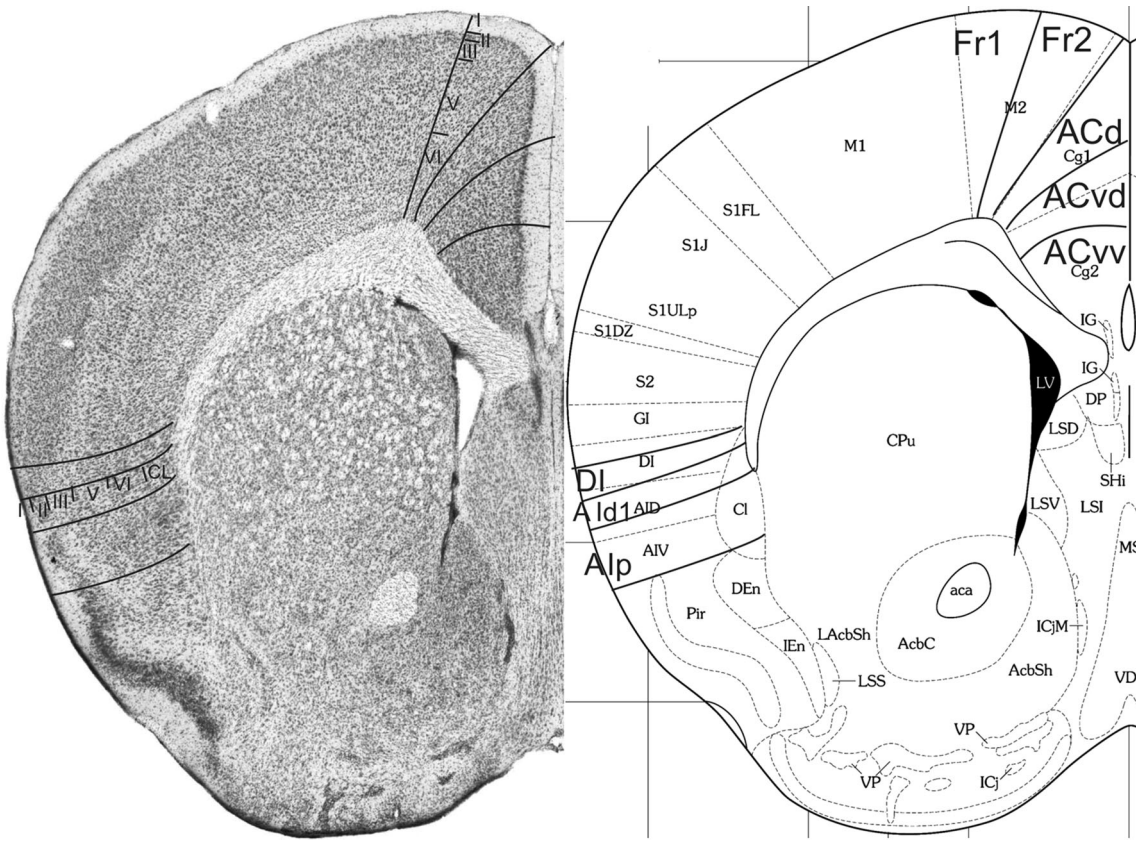

Fig. 8 Implementation of 'Van de Werd et al. (2010)' boundaries at Bregma 1.18 mm (adapted from Franklin and Paxinos 2008)

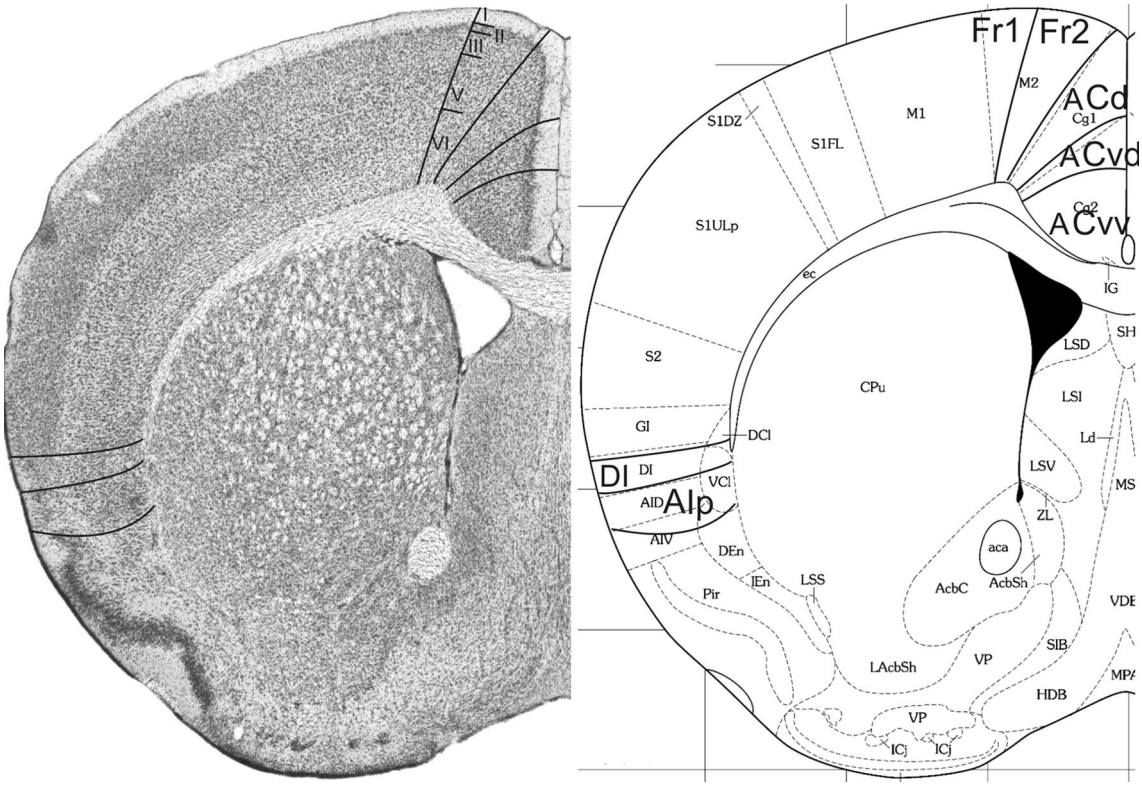

Fig. 9 Implementation of 'Van de Werd et al. (2010)' boundaries at Bregma 0.74 mm (adapted from Franklin and Paxinos 2008)

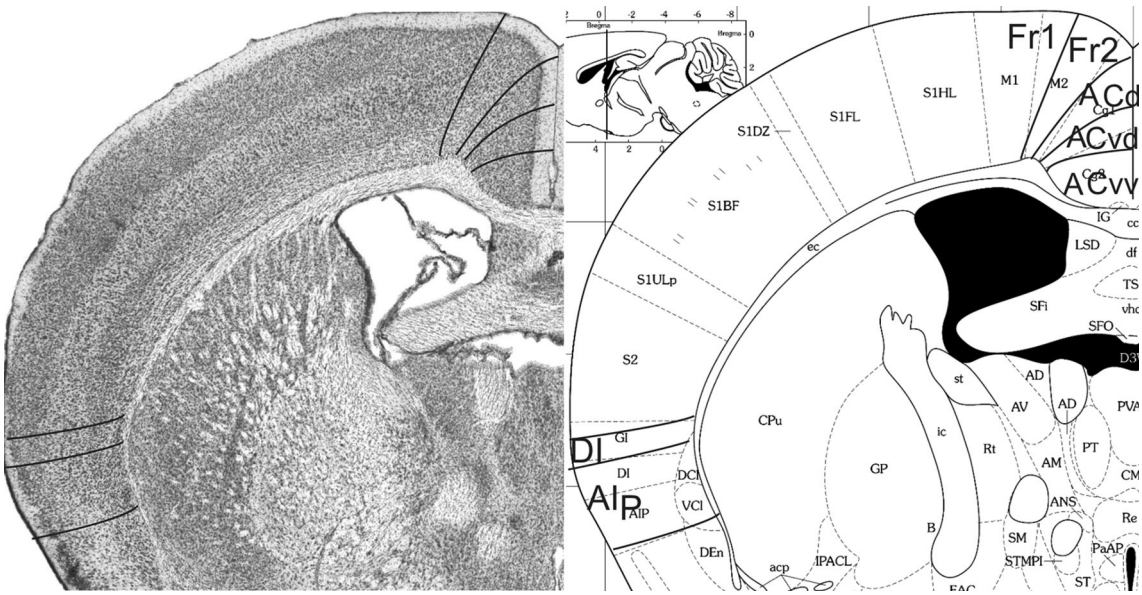

Fig. 10 Implementation of 'Van de Werd et al. (2010)' boundaries at Bregma −0.46 mm (adapted from Franklin and Paxinos 2008)

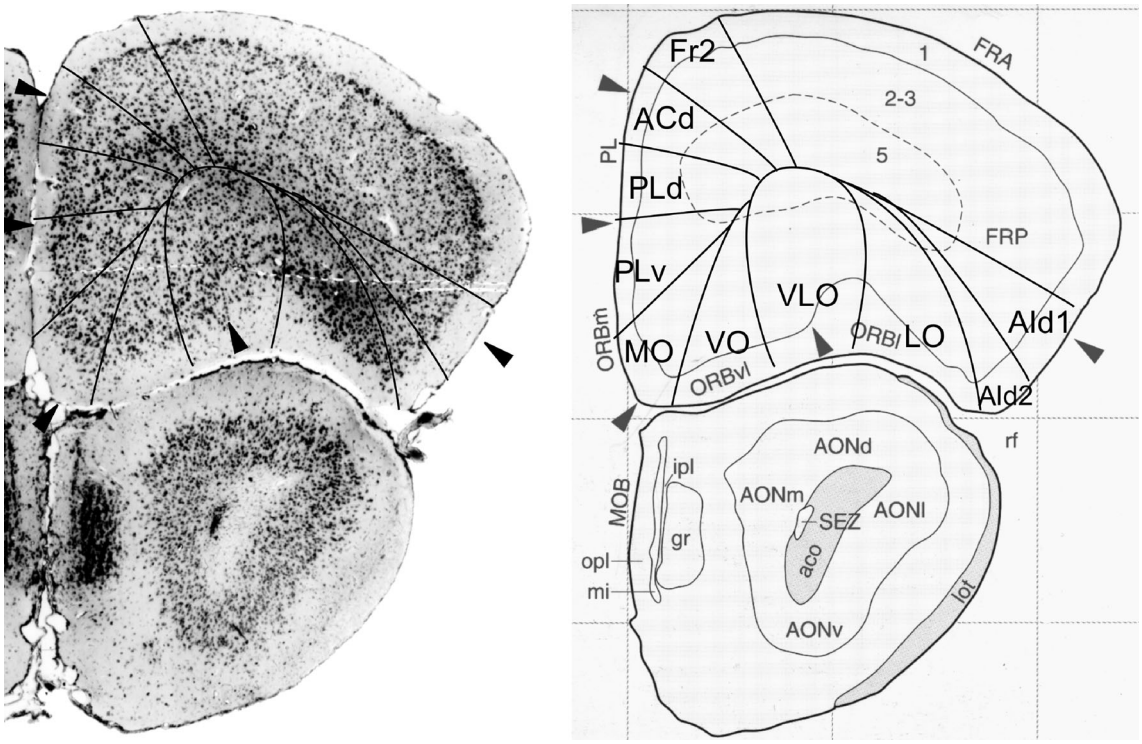

Fig. 11 Implementation of 'Van de Werd et al. (2010)' boundaries at Bregma 2.50 mm (adapted from Hof et al. 2000)

Bregma −1.10 mm (Fig. 19): In contrast with the atlas, in this figure we recognize the retrosplenial region, as the typical granular layer II of the granular retrosplenial area (**RSG**) is identifiable at this level. The **RSG** here corresponds with *ACv*. The dorsal boundary of the agranular retrosplenial area, **RSA** is defined in area *MOs*, mainly by the short distance of layer V from the pial surface, due to the absence of layer IV.

Summary

In nearly all sections, area **ACd** is equal to area *ACd* (Figs. 12, 13, 15, 16, 17, 18). Area **Fr2** is equal to the medial part of area *MOs*. The combined areas **ACvd** and **ACvv** are equal to the area *ACv* in the atlas (Figs. 17, 18). Differences in size are visible between the areas *ORBm* and **MO** (Figs. 11, 12), and between *IL* and **IL**

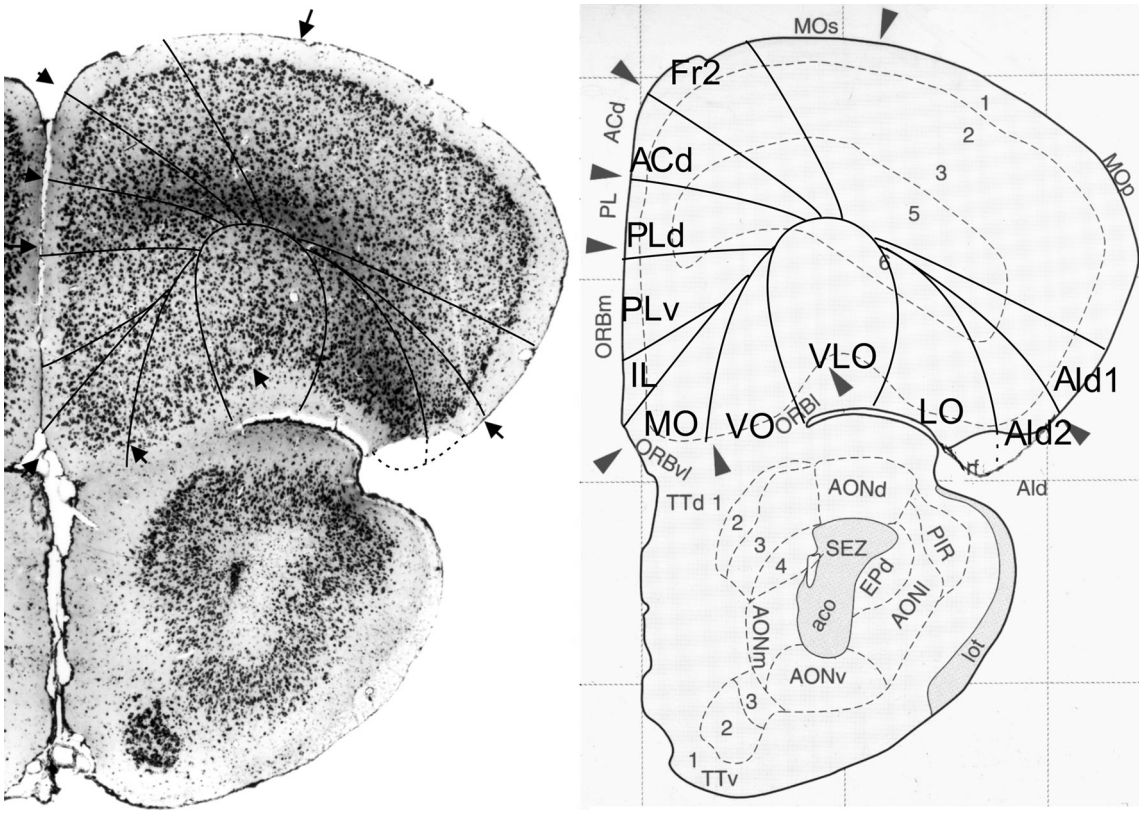

Fig. 12 Implementation of 'Van de Werd et al. (2010)' boundaries at Bregma 2.40 mm (adapted from Hof et al. 2000)

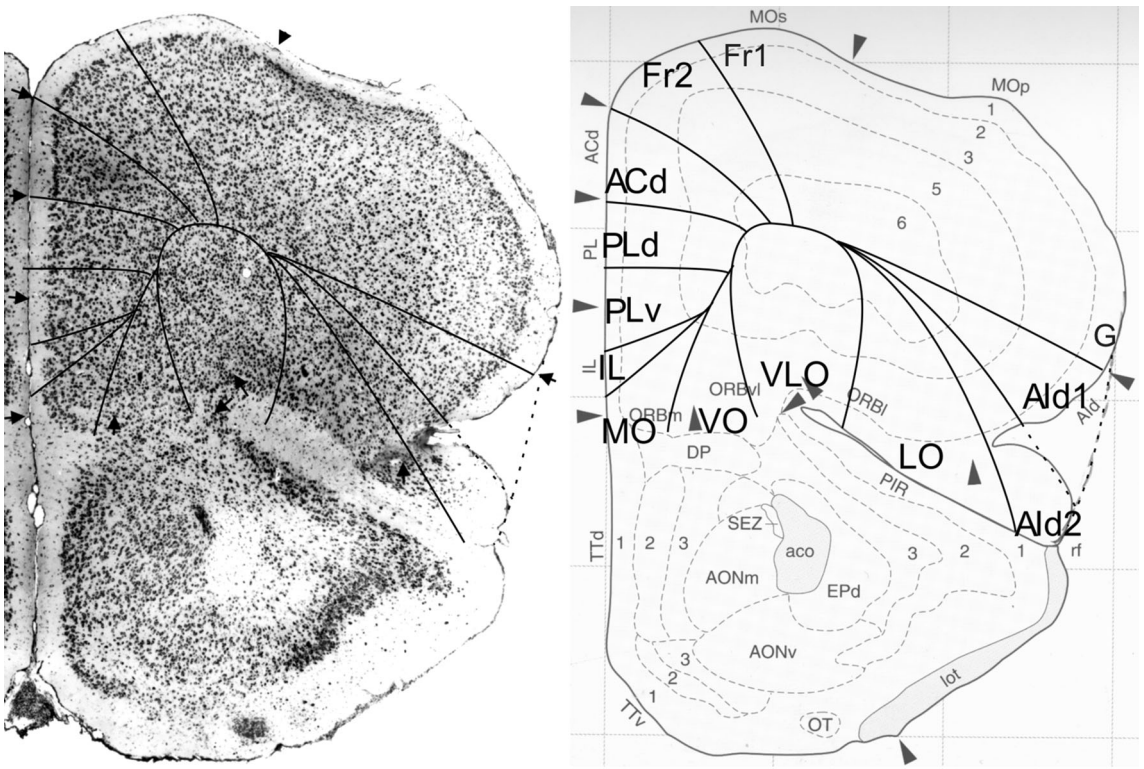

Fig. 13 Implementation of 'Van de Werd et al. (2010)' boundaries at Bregma 2.00 mm (adapted from Hof et al. 2000)

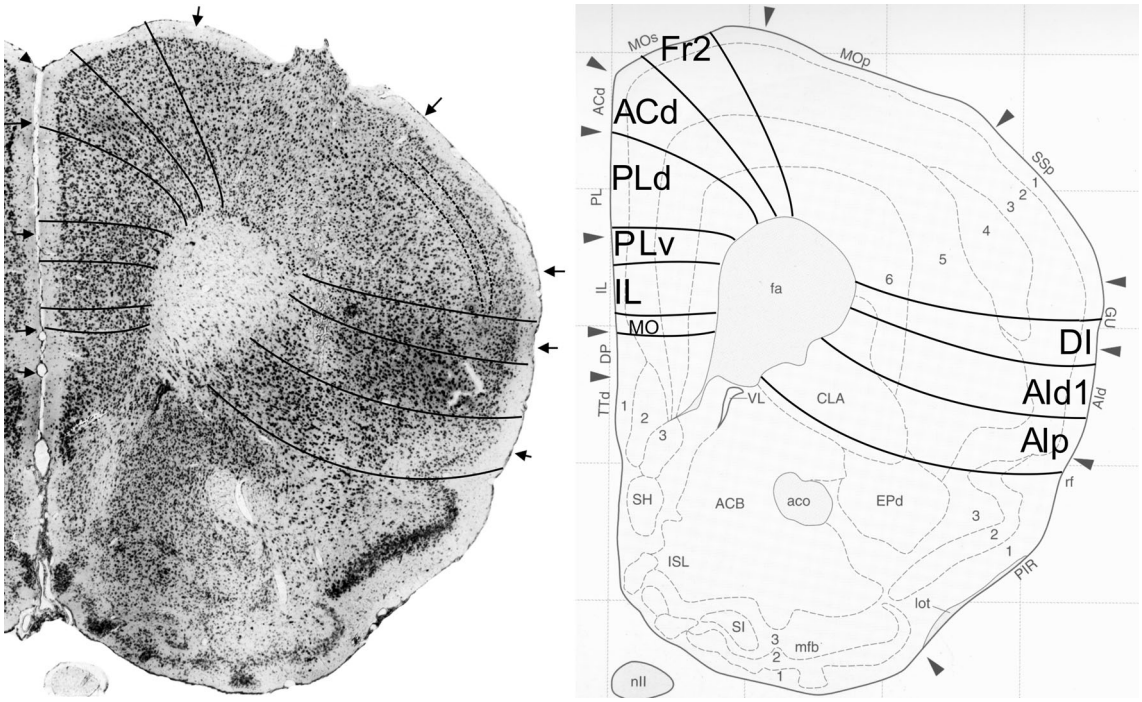

Fig. 14 Implementation of 'Van de Werd et al. (2010)' boundaries at Bregma 1.60 mm (adapted from Hof et al. 2000)

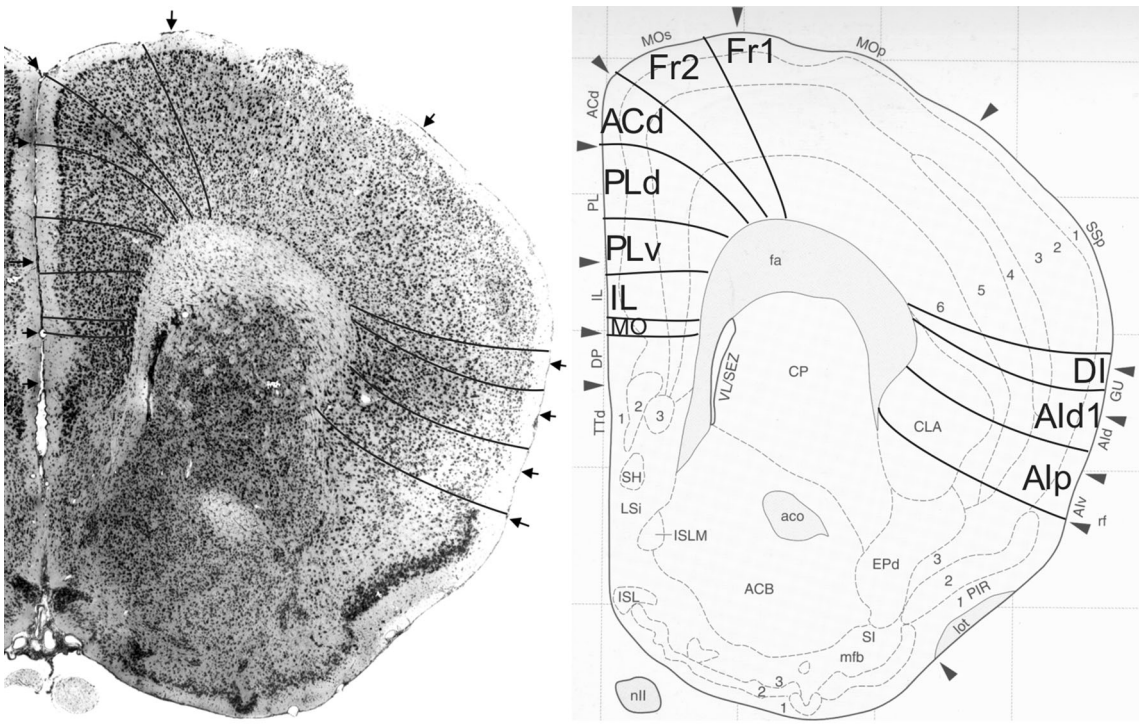

Fig. 15 Implementation of 'Van de Werd et al. (2010)' boundaries at Bregma 1.40 mm (adapted from Hof et al. 2000)

(Figs. 13, 14, 15, 16), as *ORBm* and *IL* are much larger than **MO** and **IL**, respectively. In the atlas *ORBm* (Figs. 11, 12) is replaced by *IL* posteriorly (Fig. 14, 15, 16). In our parcellation, the areas **MO** and **IL** are nearly always both visible in a section. In the atlas, the ventral orbital area is not recognized as a separate area. The

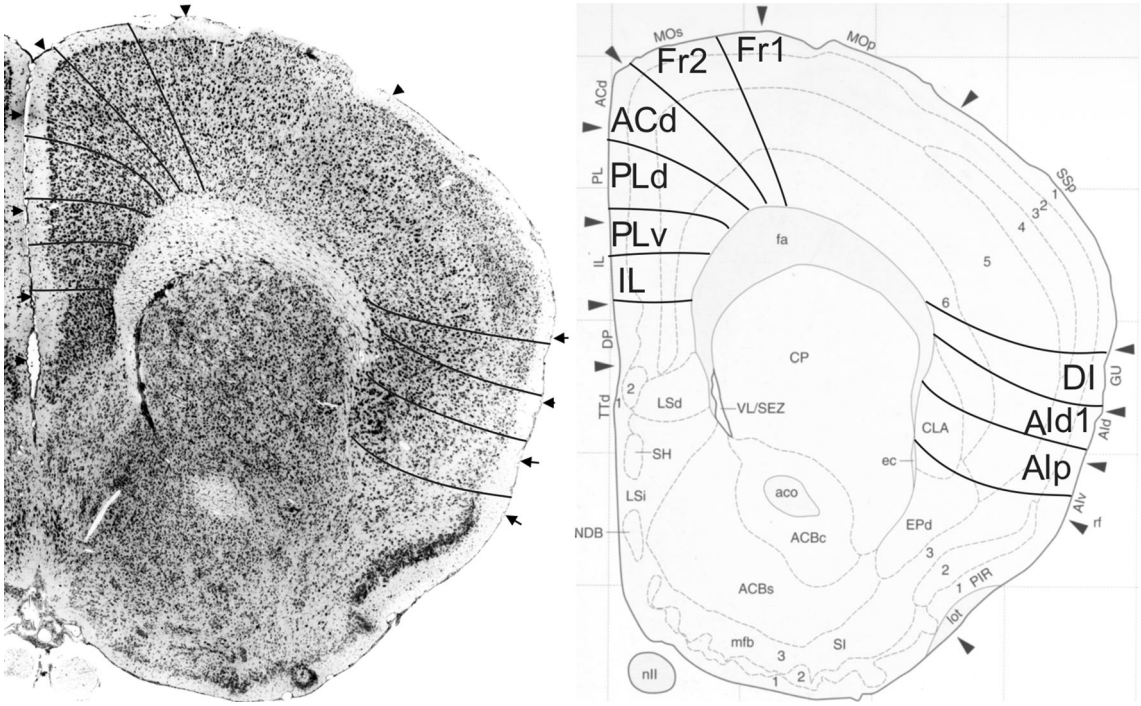

Fig. 16 Implementation of 'Van de Werd et al. (2010)' boundaries at Bregma 1.30 mm (adapted from Hof et al. 2000)

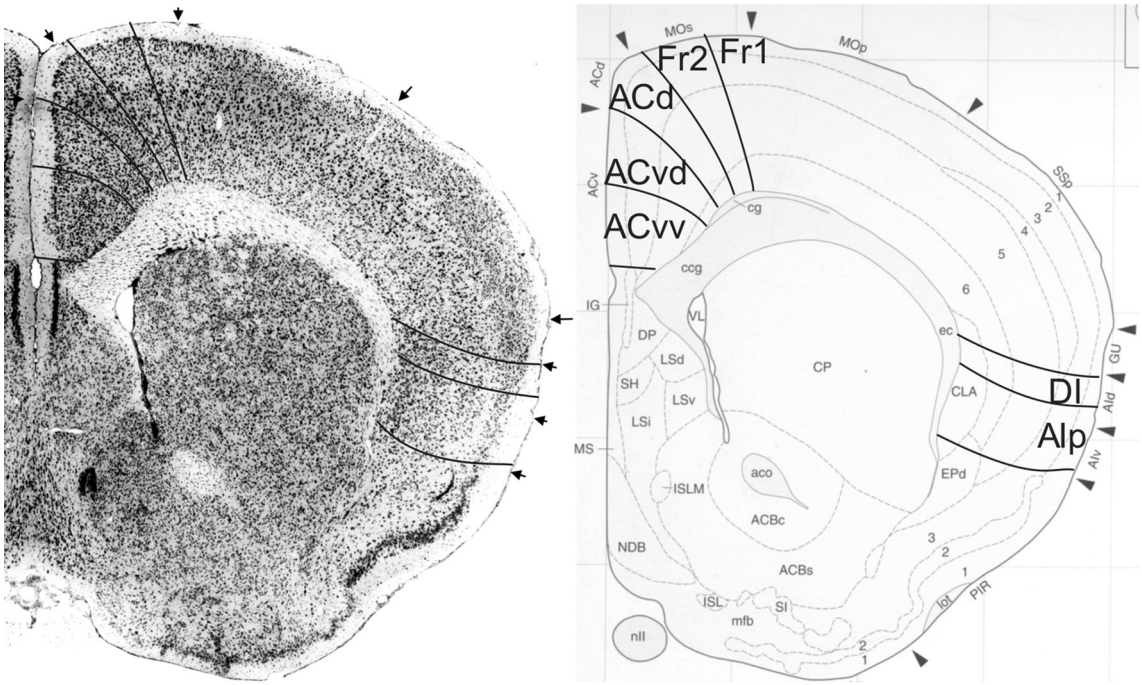

Fig. 17 Implementation of 'Van de Werd et al. (2010)' boundaries at Bregma 1.10 mm (adapted from Hof et al. 2000)

correspondence of ventrolateral area *ORBvl* varies in the atlas in each figure: in Fig. 11 with **VO** and parts of **VLO** and **MO**; in Fig. 12 with **MO**; in Fig. 13 with **VO** and **VLO**.

Comparison with the parcellation by Rose (1929)

Because of the excellent quality of the figures and the description of the cytoarchitecture, the atlas of Rose is

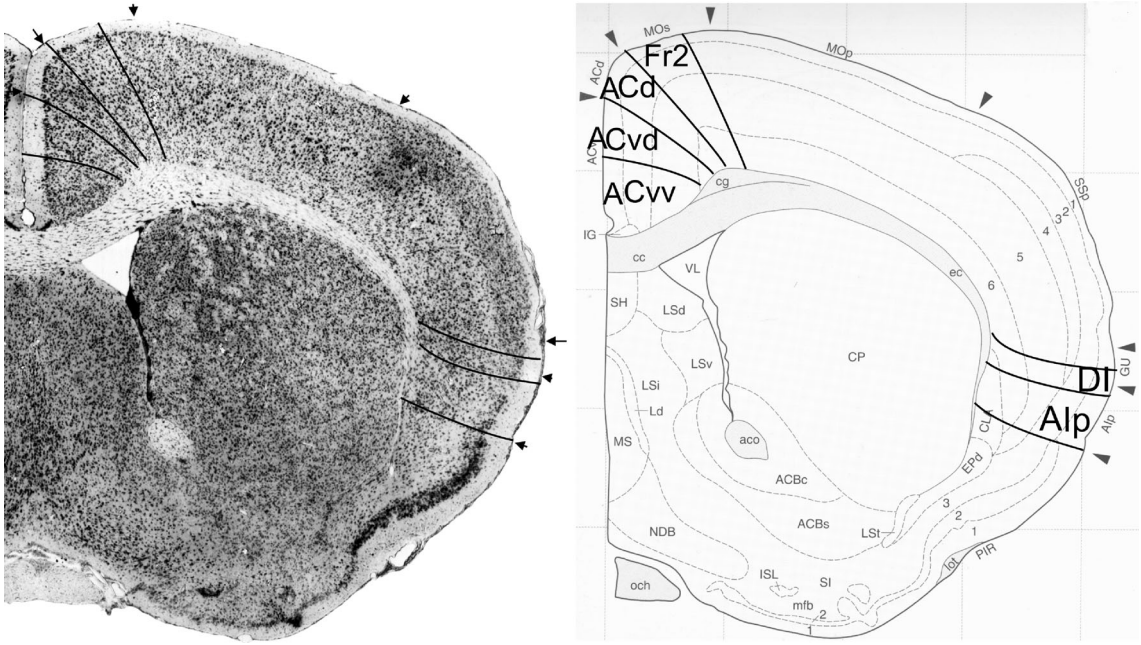

Fig. 18 Implementation of 'Van de Werd et al. (2010)' boundaries at Bregma 0.70 mm (adapted from Hof et al. 2000)

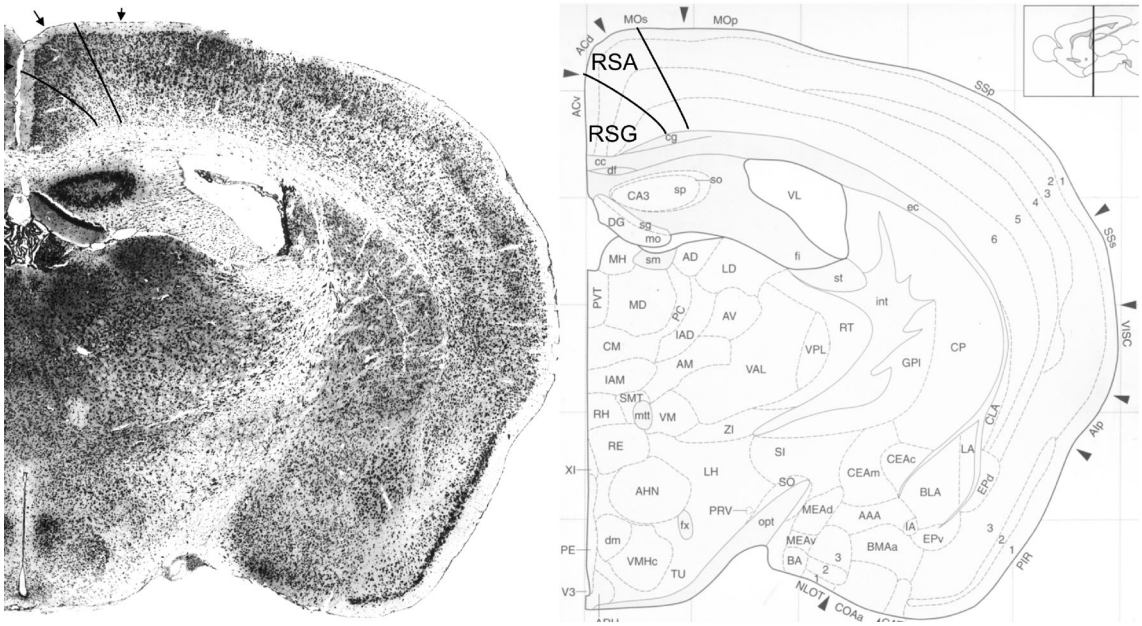

Fig. 19 Implementation of 'Van de Werd et al. (2010)' boundaries at Bregma −1.10 mm (adapted from Hof et al. 2000)

worth discussing. In the atlas of Rose (1929) boundaries are indicated by arrows placed at the surface.

Frontal lobe anterior to forceps minor

In Fig. 20 the medial boundary of **Fr2** is approximately comparable with a border indicated by Rose, as is also the ventral boundary of **PLv**. The agranular **Fr2** is located in the part of the cortex that is mentioned as granular cortex by Rose. On the lateral cortex, however, we define the dorsal boundary of the agranular insular area ventral to the boundary between the granular and agranular cortex in the Rose atlas, thus considering the dorsal part of the Rose area *ai 1* as belonging to the granular cortex. We based the dorsal boundary **AId1** on the cellular columns, the broad, densely packed layer II and the near distance of layer V to

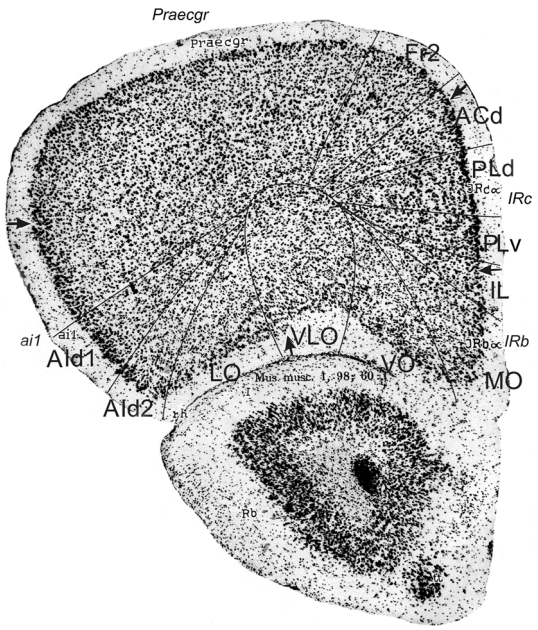

Fig. 20 Implementation of 'Van de Werd et al. (2010)' boundaries in section through frontal lobe anterior to forceps minor of Rose (1929)

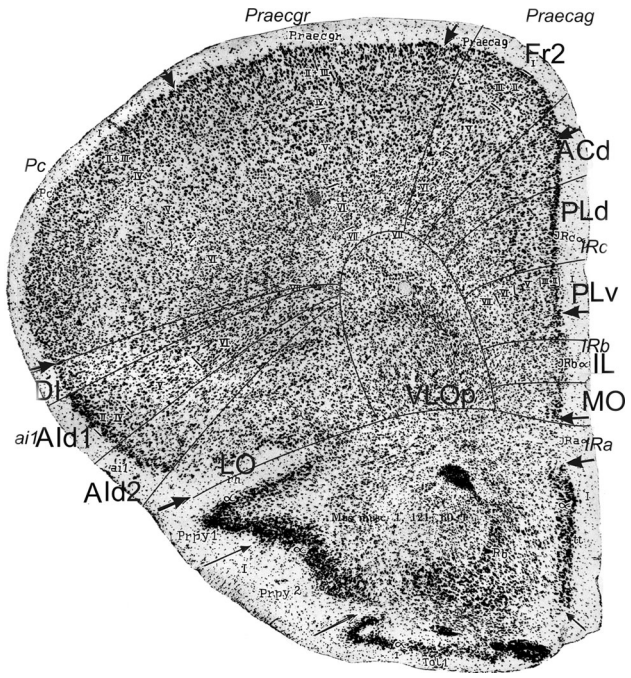

Fig. 21 Implementation of 'Van de Werd et al. (2010)' boundaries in section through frontal lobe near forceps minor of Rose (1929)

the cortical surface. The medial boundary of *ai 1* corresponds to the lateral boundary of **VLO**. Rose defined only one or two ventral PFC areas at this level.

At the coronal level of Fig. 21, the extent of the agranular cortex is similar in our parcellation to the extent of the agranular cortex in the Rose parcellation. The medial PFC areas are well definable on the basis of our criteria. Area **Fr2** is smaller and positioned between the boundaries of *Praecag*. This is probably caused by a slightly different appreciation of characteristics, such as our preference for the location of the change in the position of layer V at the lateral boundary of **Fr2**, and, at the medial boundary of **Fr2**, our choice for the difference in the packing density of the cellular columns in determining boundary **Fr2/ACd**. Here, areas **ACd**, **PLd**, **PLv**, **IL** and **MO** are rather easy to define according to the criteria specified in Appendix 1.

Frontal lobe anterior to genu of the corpus callosum

In Fig. 22, the combined areas **ACd** and **Fr2** are approximately comparable to *Praecag*. The areas **PLd**, **PLv** and **IL** are also easily definable (Appendix 1). On the lateral side of the frontal lobe, the boundary **DI/AId1** is equal to the boundary between the *anterior granular insular area* (*i 1*) and the *anterior agranular insular area* (*ai 1*). The ventral border of **AIp** is approximately the ventral border of *ai 1*. We define **AId1** in the dorsal part of *ai 1* (Appendix 1). We agree with Rose that the cells of the claustrum are larger than the cells of the cortical layer VI.

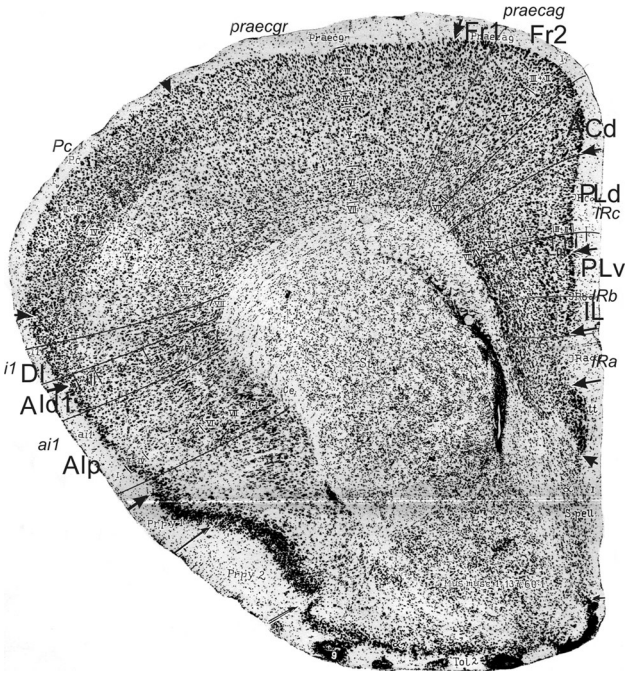

Fig. 22 Implementation of 'Van de Werd et al. (2010)' boundaries in section through frontal lobe anterior to genu of the corpus callosum of Rose (1929)

Frontal lobe dorsal to corpus callosum

In Fig. 23, we distinguish, ventrally to area **ACd**, the areas **ACvd** and **ACvv**. The difference in the packing density of

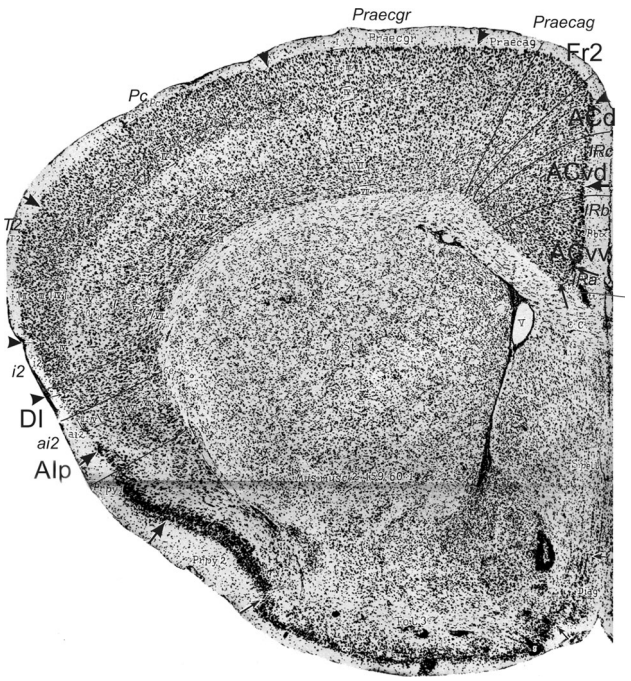

Fig. 23 Implementation of 'Van de Werd et al. (2010)' boundaries in section through frontal lobe just caudal to genu of the corpus callosum of Rose (1929)

cells is more gradual between **ACvd** and **ACvv** than between **PLd** and **PLv** in the previous sections. The ventral boundary of **ACvd** is approximately equal to a ventral boundary of Rose. On the lateral side of the frontal lobe, we distinguish the areas **DI** and **AIp** (see Appendix 1) as localized in the Rose area *ai 2*. The cytoarchitecture of **DI** is different from the cytoarchitecture of **AIp**, but in the parcellation of Rose they both are located in area *ai 2*.

Summary

In most sections, area **Fr2** agrees with a large part of the Rose *regio praecentralis agranularis* (Figs. 21, 22, 23). Correspondence is found with Rose boundaries for the boundaries **Fr1/Fr2** (Figs. 21, 22), **Fr2/ACd** (Fig. 20), **PLd/PLv** (Fig. 22), **PLv/IL** (Fig. 20), **ACvd/ACvv** (Fig. 23) and **DI/AId1** (Fig. 22).

Comparison with other mouse PFC parcellations

Caviness (1975) and Wree et al. (1983) have published studies on the boundaries of mouse cortical areas, including areas of the PFC. In both studies, a limited number of photographs are presented in which we have implemented the boundaries based on our criteria for delineating the PFC areas.

Caviness (1975)

For the denomination of mouse cortical areas Caviness (1975) has applied a numerical terminology derived from Brodmann (1909) and Krieg (1946).

In Fig. 24, in the medial PFC, it is possible to differentiate the PFC areas **Fr2** and **ACd** mainly on the basis of the packing density of the cellular columns of layers V and VI, and on the cells in **Fr2** which are larger than in **ACd**, rather than on the differences in layer II. Most of area **Fr2** is in *field 8*. In *field 24*, at least three different areas are distinguishable on the basis of the cytoarchitecture. **IL** is partly in *field 24,* and partly in *field 25*. **IL** is recognizable by the homogeneous layers II, III and V. The boundaries of **MO** are estimations because the resolution did not allow us to delineate this area with complete reliability. On the lateral side of the frontal lobe, it is difficult to compare our parcellation with the parcellation of Caviness (1975) because in the two *fields 10 and 11,* we distinguish five different areas which show only a very restricted relation with the *fields 10 and 11*.

In Fig. 25, area **Fr2** largely corresponds with *field 8*. In *field 24* areas **ACd**, **ACvd** and **ACvv** can be distinguished on the basis of the criteria described in Appendix 1. In *field 14* the areas **DI** and **AId1** are distinguishable. In *field 13* the separation between the cortical layers is characteristic of the identification of area **AIp**.

Summary

Boundary **Fr2/ACd** is nearly equal to the boundary between the *fields 8* and *24* (Figs. 24, 25). Boundary **PLv/IL** is

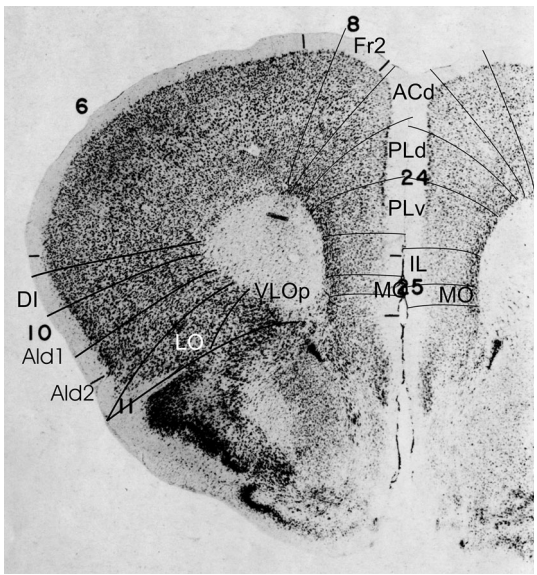

Fig. 24 Implementation of 'Van de Werd et al. (2010)' boundaries in section through forceps minor of Caviness (1975)

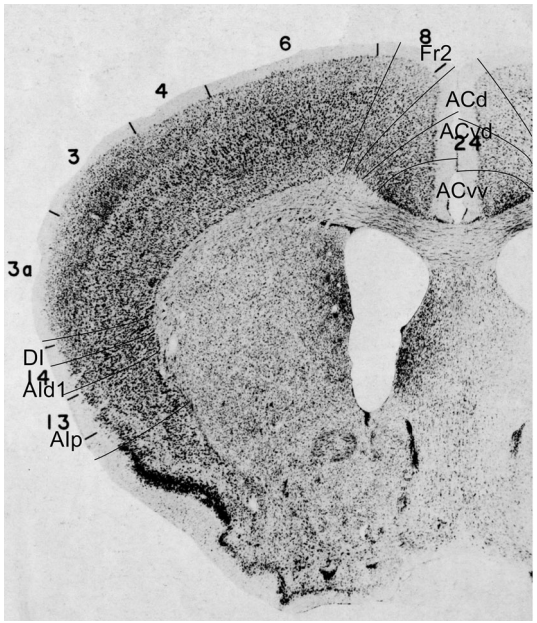

Fig. 25 Implementation of 'Van de Werd et al. (2010)' boundaries in section through frontal lobe dorsal to corpus callosum and anterior to hippocampus of Caviness (1975)

approximately equal to the boundary between the *fields 24* and *25* (Fig. 24). Boundary **AId1/AIp** is nearly equal to the boundary between the *fields 14* and *13* (Fig. 25).

Most of the other boundaries in this paper are not comparable to the boundaries in our parcellation.

Wree et al. (1983)

Wree et al. (1983) compare Nissl-stained sections with the images generated by the GLI. Boundaries are only presented in the GLI images and indicated by arrow heads.

We have delineated boundaries according to our parcellation system in the Nissl micrograph and subsequently copied them in the GLI image.

In Fig. 26, the areas of the medial PFC as well as the areas in the lateral PFC are clearly distinguishable in the Nissl micrographs according to the criteria specified in Appendix 1. The combined areas **PLv**, **IL** and **MO** correspond to *cingulate area 4* (*C4*), the areas **ACd** and **PLd** approximately to the *cingulate area 1* (*C1*). Wree et al didn't specify different areas in the lateral PFC, but in this figure the whole *claustrocortex, Cl,* corresponds to **DI, AId1** and **AIp** together.

In Fig. 27, the lateral boundary of **Fr2** is approximately the lateral boundary of the *medial precentral area Prcm*. *Prcm* roughly encompasses both **Fr2** and **ACd**. Boundary **ACd/ACvd** (see Appendix 1) is approximately boundary *Prcm/C1*. Boundary **ACvd/ACvv** (see Appendix 1) is equal to boundary *C1/C2*. Dorsally to the corpus callosum the *cingulate areas 1 and 2* coincide with **ACvd** and **ACvv**, respectively. At this level, the whole *claustrocortex, Cl,* in the lateral side of the frontal lobe approximately encompasses **DI** and **AIp**.

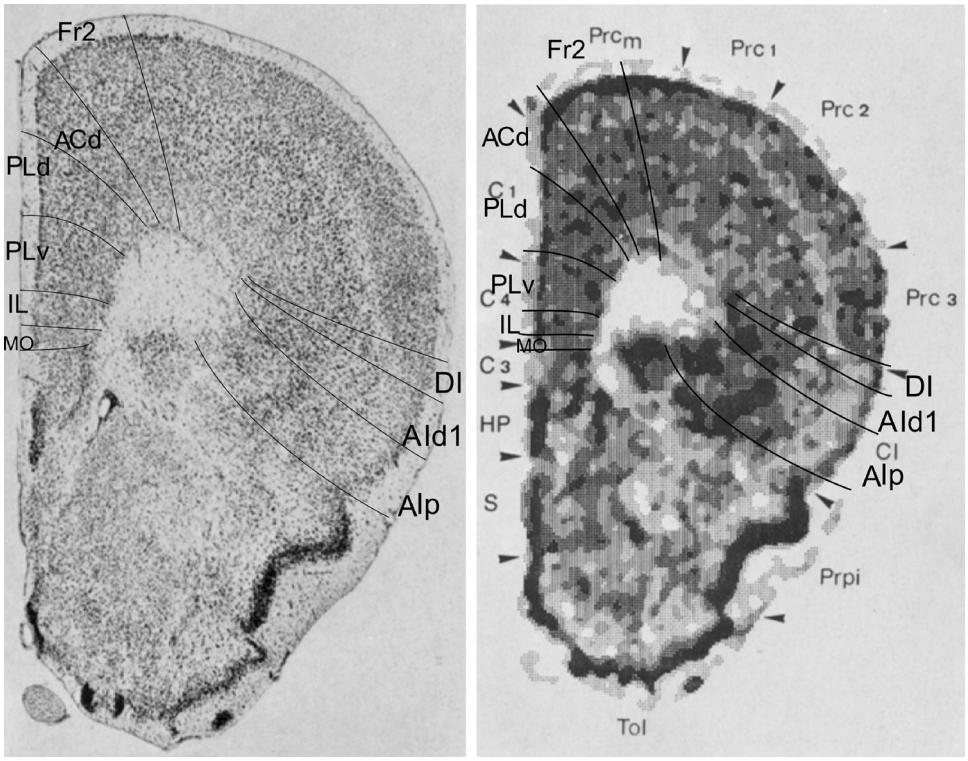

Fig. 26 Implementation of 'Van de Werd et al. (2010)' boundaries in section through forceps minor of Wree et al. (1983)

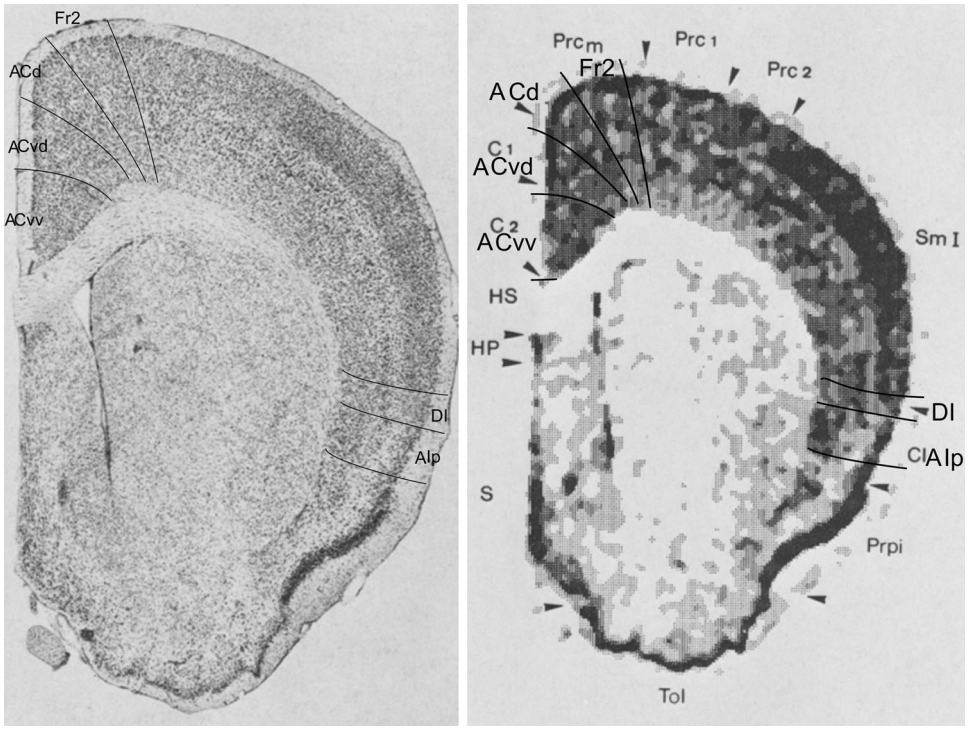

Fig. 27 Implementation of 'Van de Werd et al. (2010)' boundaries in section through frontal lobe dorsal to corpus callosum and anterior to hippocampus of Wree et al. (1983)

Summary

The boundary **PLd/PLv** is equal to the boundary *C1/C4* (Fig. 26). In Fig. 26, boundary **Fr2/ACd** is approximately equal to boundary $Prc_m/C1$. In Fig. 27, boundary **ACd/ACvd** is nearly equal to boundary Prc_m/C1 and boundary **ACvd/ACvv** is equal to boundary *C1/C2*. In Fig. 26 the combined areas of **DI**, **AId1** and **AIp** are equal in size to the claustral cortical area (*Cl*). In Fig. 27, area **AIp** is approximately equal to the claustral cortical area (*Cl*).

Comparison summarized in tables

Comparison of the presence of boundaries between subareas

In Table 1, we have indicated to what extent the boundaries of the PFC subareas as described by Van de Werd et al. (2010) are recognized in the publications by other authors *regardless of* the terminology they have applied. Due to the fact that we were sometimes unable to delineate a particular PFC boundary in one of the available micrographs of a publication or atlas, a comparison was not always possible. We have indicated the areas in the frontal pole anterior to the forceps minor before the symbol '/', and the areas caudal to the tip of the forceps minor after the symbol '/'.

In the publications of Caviness (1975) and Wree et al. (1983), boundaries are only shown in coronal sections caudal to the tip of the forceps minor.

Table 1 indicates that many boundaries show broad agreement with at least one of the publications reviewed and that a few show considerable agreement in at least two atlases, i.e. **Fr2/ACd**, **ACd/PLd**, **ACd/ACvd**, and **AId2/LO**.

Comparison of location and extent of subareas

Tables 2 and 3 show the relationship between Van de Werd et al. (2010) areas and areas in the stereotactic atlases reviewed. The original terminology is maintained in the tables. Table 2 considers the frontal lobe anterior to the tip of the Forceps minor, and Table 3 the frontal lobe caudal to the tip of the Forceps minor.

In Table 2, the delineations of PFC areas differ widely in the frontal pole. It is only just before the forceps minor that correspondence is found for area **ACd** with the comparable area *Cg1* in the Franklin and Paxinos (2008) atlas as well with the comparable area *ACd* in the Hof et al. (2000) atlas. Further, correspondence is found just rostral to the forceps minor for the Van de Werd et al. (2010) areas **PL** (i.e. **PLd** + **PLv**), **LO** and **VLO** with areas *Cg2*, *LO* and *VO*, respectively, in the atlas of Franklin and Paxinos (2008), and with area *ORBl* in the atlas of Hof et al. (2000). Also the combined areas **AId1** and **AId2** are comparable with the Hof et al. (2000) area *AId* just rostral to the tip of the forceps minor. The atlas of Franklin and Paxinos (2008) and the atlas of Hof et al. (2000) show a good mutual correspondence between the secondary motor areas *M2* and *MOs*, and for the medial

Table 1 Comparison boundaries anterior and posterior to tip of the forceps minor

Van de Werd et al. (2010)	Franklin and Paxinos (2008)	Hof et al. (2000)	Rose (1929)	Caviness (1975)	Wree et al. (1983)
Fr1/Fr2	$^{+}$–/–	–/∼	$^{-}$+/∼	/∼	/∼
Fr2/ACd	$^{-}$+/+	$^{\sim}$+/+	$^{-}$∼/∼	/+	/∼
ACd/PLd	$^{-}$+/+	$^{-}$+/+	–/+	/–	/–
PLd/PLv	$^{+}$–/–	$^{+}$–/∼	–/∼	/–	/+
PLv/IL	–/+	–/∼	–/–	/–	/–
PLv/MO		–/	–/		
IL/MO or IL/DP	–/–	+/+	–/+	/+	/+
MO/DP	∼/∼	/+	∼/+	/∼	/+
MO/VO	$^{+}$–/	∼/	–/		
VO/VLO	$^{-}$+/	–/	–/		
VLO/LO	$^{-}$∼/	–/	∼/		
ACd/ACvd	/+$^{\sim}$	/+	/–	/–	/+
ACvd/ACvv	/–$^{+}$	/–	/+	/–	/+
GI/DI	∼/∼	/∼	+/∼	/∼	/∼
GI/AId1 or DI/AId1	+/∼	∼/+	–/∼	/–	/∼
AId1/AId2	$^{-}$∼/–	–/	–/	/–	
AId2/LO	$^{-}$+/–	$^{-}$+/	$^{-}$+/	/–	
DI/AIp	/∼	/∼	/∼		/+
AId1/AIp	/∼	/+	/∼	/∼	/+

/, separation region anterior and posterior to tip of forceps minor; +, good correspondence of boundary; ∼, boundary approximately equal; –, no correspondence; symbols in superscript in front of '/' regard the most rostral section(s); symbols in superscript after '/' regard most caudal section(s); no symbol, boundary not indicated

Table 2 Comparison of PFC areas anterior to the forceps minor

Van de Werd et al. (2010)	Franklin and Paxinos (2008)	Hof et al. (2000)
Medial		
Fr2	*≪PrL → <<<FrA →* ≪M2	*<<<FRA → ≪MOs*
ACd	*≪PrL → ≈ Cg1*	*<<<FRA + ≪PL → ≈ACd*
PLd + PLv	*≪PrL + ≪MO → ≈PrL*	*<PL + <ORBm → ≈PL + ≪IL*
PLd	*≪PrL → <PrL*	*<PL*
PLv	*≪MO → <PrL + ≪MO*	*<ORBm → ≪PL + ≪IL*
IL	*<<<MO*	*≪ORBm → ≪IL*
MO	*≪MO*	*≪ORBm + <<<ORBvl → ≈ORBvl → ≈ORBm*
Lateral		
AId1 + AId2	*<DLO + <<<LO → <AID + <AIV*	*<<<ORBl + <<<FRA → <<<MOp + ≪AId → ≈AId*
AId1	*≪DLO + <<<LO → <AID*	*<<<ORBl + <<<FRA → <<<MOp → <AId*
AId2	*≪DLO + <<<LO → <AIV + ≪AID*	*<<<ORBl → ≪AId*
Ventral		
LO	*≪DLO + <LO → ≈LO*	*<ORBl → <AID → <ORBl*
VLO	*≪LO + ≪VO → ≈VO*	*≪ORBvl + <<<ORBl → ≪ORBl + <<<AId → ≪ORBvl* + ≪ORBl
VO	*<VO → ≪VO → <<<MO*	*<ORBvl → <ORBl → <<<ORBm + ≪ORBvl*

<<<, 'Van de Werd et al.' area is a very small part of; ≪, VdW-area is a small part of; <, VdW-area is a large part of; ≈, VdW-area is equal or approximately equal to; +, together with; →, this changes in caudal direction into

orbital areas *MO* in these atlases at Bregma 2.58 and 2.34 mm, and *ORBm* at Bregma 2.50 and 2.40 mm, respectively.

In Table 3 the relation of the areas **Fr2** and **ACd** in Van de Werd et al. (2010) to areas in the atlases of Franklin and Paxinos (2008) and Hof et al. (2000) is very stable, as is

Table 3 Comparison of PFC areas posterior to tip forceps minor

Van de Werd et al. (2010)	Franklin and Paxinos (2008)	Hof et al. (2000)
Medial		
Fr2	*<M2*	*<MOs*
ACd	*≈Cg1*	*≈ACd*
PLd + PLv	*≈PrL → ≈PrL + ≪IL → ≈Cg2*	*≈PL + ≪IL → ≈PL → ≈PL + ≪IL*
PLd	*<PrL → <<<Cg1 + ≪Cg2*	*≈PL → <PL*
PLv	*<PrL → ≪PrL + ≪IL → <Cg2*	*≪IL → ≪PL → ≪IL*
ACvd + ACvv	*≪Cg1 + ≈Cg2 → ≈Cg2*	*≈ACv*
ACvd	*≪Cg1 + ≪Cg2 → ≪Cg2*	*<ACv*
ACvv	*<Cg2*	*<ACv*
IL	*<IL → ≪IL*	*<IL*
MO	*≪IL*	*<<<IL*
Lateral		
DI	*<AID → ≈GI → ≈DI → ≈GI*	*≈GU → ≪AId → <GU*
AId1 + AId2	*≪AID + ≈AIV + <LO*	*≈AId*
AId1	*≪AID + <AIV → ≈DI → <AID*	*≪AId → <AId + ≪GU → ≈AId*
AId2	*≪AIV + <LO*	*≪AId*
AIp	*<AIV + ≪LO → ≈AIV + ≪AID → ≪AIV + ≈AID → ≈DI + ≈AIP*	*≪AId → ≈AIv + ≪AId → ≈AIp*

<<<, 'Van de Werd et al.' area is a very small part of; ≪, VdW-area is a small part of; <, VdW-area is a large part of; ≈, VdW-area is equal or approximately equal to; +, together with; →, this changes in caudal direction into

seen in successive figures. Equal location is only found for area **ACd** and areas *Cg1* and *ACd*, respectively. The combined Van de Werd et al. (2010) areas **ACvd** and **ACvv** correspond with area *ACv* in Hof et al. (2000). The transition of the prelimbic cortex to the ventral part of the anterior cingulate cortex is at Bregma 1.42 in Franklin and Paxinos (2008), after Bregma 1.30 in Hof et al. (2000) and Van de Werd et al. (2010). The Franklin and Paxinos (2008) area *AIV* at Bregma 1.42 mm is equal to the Hof et al. (2000) area *AIv* at Bregma 1.42 mm. The anterior boundary of the posterior agranular insular area (**AIp**) in Van de Werd et al. (2010) is more rostral than the anterior boundary of this area in Franklin and Paxinos (2008) and Hof et al. (2000). This may be explained by a difference in cytoarchitectonic criteria used. Fluctuation in the position of areas in the ventral side of the frontal lobe is visible in Hof et al. (2000). Table 2 shows that in general no stable relation is found in position and size between ventral areas that are specified in the different parcellations studied.

Discussion

The aim of this study has been to review the similarities and differences that are met in the parcellation of the mouse PFC by different investigators. Clarity about the anatomical substrate of the PFC is important to avoid miscommunication in the evaluation of results obtained by tracing, morphometric, lesion and neurophysiological studies.

As extensive series of coronal sections of the PFC are only found in the atlases, we will mainly discuss the difference between the parcellation in the atlases, particularly the Franklin and Paxinos atlas, and the Van de Werd et al. boundaries. The Results show that miscommunication is quite likely, since we have detected that (a) different terms are used for the same cortical structure and (b) cortical areas specified by a comparable term may have different locations/extents.

Some examples of different naming of the same cortical structure are the following ones. The term 'ventrolateral orbital area' **VLO** lacks in the atlas of Franklin and Paxinos, while *DLO* lacks in Van de Werd et al. The term 'dorsal agranular insular area, ventral part (**AId2**) and the term 'agranular insular cortex, ventral part' (*AIV*) are applied for the same part of the cortex on the lateral side of the frontal lobe. The terms 'area **Fr2**', 'secondary motor cortex (*M2* or *MOs*)', 'precentral agranular area (*Prcag*)', 'cortical *field 8*' and 'medial precentral area (Prc_m)' are used to indicate the dorsomedial PFC subarea, which, among other things, is involved in eye movements. It has to be pointed out that **Fr2** differs in extent largely from areas *M2* and *MOs*.

Some examples of cortical areas specified by comparable names which have different locations/extents are the following. The difference between extension and location of **ACd** and *Cg1* results in a definition of 'dorsal anterior

cingulate area' **ACd** in the medial crown of the frontal pole at a location within the 'prelimbic area' *PrL* specified by Franklin and Paxinos. As a consequence, the extension and location of prelimbic area **PL** differ from the *PrL* area. Other examples are the 'medial orbital area (MO)' and the 'infralimbic area (IL)'. The extent of the areas *MO* and *IL* is large in the stereotactic atlases, while both **MO** and **IL** are quite restricted in the 'Van de Werd et al.' parcellation.

The '*ventrolateral orbital area ORBvl*' in the Hof et al. (2000) atlas and the '*ventral orbital area VO*' in the Franklin and Paxinos (2008) atlas differ in location and extent from the 'ventrolateral area' **VLO** and 'ventral orbital area' **VO** in the 'Van de Werd' parcellation, respectively. Some of the differences in parcellation can be explained by the use of another staining method next to the Nissl staining. So it is clear from the atlas of Franklin and Paxinos (2008) that for the definition of the prelimbic area they probably rely on the data of acetylcholinesterase (AChE)-stained sections. This location of *PrL* generally agrees with our **PL**, but differs at the "most frontal" sections (Figs. 1, 2). We have consequently used the same criteria to define **PL**, also in the most frontal sections. In addition, Van de Werd et al. defined a distinction between a dorsal and a ventral part in the prelimbic area (**PL**). This is corroborated by studies in the mouse by Rose (1929), Wree et al. (1983) and Van de Werd et al. (2010) and by studies in the rat by Heidbreder and Groenewegen (2003), Groenewegen and Uylings (2010) and Van de Werd and Uylings (2008). The distinction between a dorsal and a ventral part in **ACv** (Van de Werd et al. 2010) looks a rather new subdivision, but a discrimination between **ACvd** and **ACvv** has been made before by Rose (1929) and Wree et al. (1983), see Figs. 23 and 27.

In the mouse, Franklin and Paxinos (2008) distinguish the dorsolateral orbital area (*DLO*) anterior to the agranular insular areas (*AID*) and (*AIV*). This distinction is not made in the other atlases and publications on mouse brain as reviewed in this study. In the rat prefrontal cortex, however, the dorsolateral orbital area (**DLO**) has been considered as an area that is functionally and cytoarchitectonically different from the agranular insular areas (e.g., Ray and Price 1992; Van de Werd and Uylings 2008; Groenewegen and Uylings 2010; Hoover and Vertes 2011). In the mouse we could not define a **DLO**.

In the rat, Van Eden and Uylings (1985), Ray and Price (1992), and Van de Werd and Uylings (2008) distinguished the ventral agranular insular area (**AIv**) on the dorsal bank of the rhinal fissure, but we were unable to distinguish **AIv** on the dorsal bank of the mouse. In the mouse we defined the dorsal bank of the rhinal fissure largely as **LO**. Given the observed cytoarchitectonic features, we do not consider the mouse area **AId2** to be equivalent with the rat area **AIv** (Van de Werd and Uylings 2008), but with the rat area **AId2**. Just before the forceps minor this region has been specified as *AIV* by Franklin and Paxinos (2008). On the ventral side of the frontal lobe, the distinction of both subareas, **VLO** and **VO** is corroborated by cytochemical characteristics in the mouse (Van de Werd et al. 2010) and supported by the tracing studies in the rat (Groenewegen 1988; Ray and Price 1992; Reep et al. 1996; Schilman et al. 2008).

Descriptions of the cytoarchitecture of areas in the region of the PFC were also published by Caviness (1975), De Vries (1912) and Tsuneda (1937). The latter two authors, however, illustrate the cytoarchitecture only in restricted parts in their studies, so that the boundaries could not be evaluated and, therefore, are not discussed any further. The cytoarchitectonic criteria used by Caviness (1975) are more detailed, but only a few figures are presented with fewer subareas than observed in the Van de Werd et al. (2010) parcellation.

The boundaries we implemented on the original photographs were based on the criteria described in Van de Werd et al. (2010) and summarized in Appendix 1. Overall these criteria could well be applied to the photographs. In a photograph, however, boundaries are more difficult to assess than when the sections are examined under the microscope. The limitation of the examination in a photograph and the limited number of photographs presented in some publications may be responsible for less precise boundaries in those photographs where the Van de Werd et al. criteria could not be fully applied. Especially, the most rostral cross-sectional boundaries had to be partly extrapolated from more caudal cross-sections. We only selected Nissl-stained photographs which contained PFC areas, for the assessment of boundaries in the PFC. The Nissl staining is preferred to delineate the PFC boundaries (Van de Werd et al. 2010; Paulussen et al. 2011), because Nissl staining has proved to be superior to any other staining in visualizing boundaries in general (Van de Werd and Uylings 2008; Van de Werd et al. 2010; Uylings et al. 2010). The Nissl staining is also the staining generally applied in morphometric studies, tracing studies and physiological studies for defining the location of an electrode.

In the atlases and publications reviewed, five different mouse strains have been studied. With the assistance of the criteria described in Appendix 1 all PFC areas could be defined in these five strains.

Our cytoarchitectonic descriptions focus upon the characteristics at the boundaries (Van Eden and Uylings 1985; Uylings and Van Eden 1990; Van de Werd and Uylings 2008; Van de Werd et al. 2010; Uylings et al. 2010) in contrast to the generally applied procedure of describing cytoarchitectonic characteristics of whole subareas. In addition, we used the requirement that the boundaries are described in such a way that on the basis of these descriptions the boundaries can be reproducibly

positioned by students of PFC. It is worth mentioning that a previous, comparable cytoarchitectonic approach (Van Eden and Uylings 1985; Uylings and Van Eden 1990; Van de Werd and Uylings 2008) has resulted in a parcellation of rat PFC that better 'fits' the tracing/connectivity studies with the compartments in the thalamic mediodorsal nucleus, the thalamic midline and intralaminar nuclei, the basal ganglia and amygdala (e.g., Groenewegen 1988; Groenewegen et al. 1990; Schilman et al. 2008; Groenewegen and Uylings 2010; Hoover and Vertes 2011), and functional studies (e.g., Heidbreder and Groenewegen 2003; Dalley et al. 2004). Our parcellation of mouse PFC subareas is in line with the one of rat PFC subareas. Therefore, we expect that our cytoarchitectonic criteria and parcellation of the mouse PFC will be very useful for a more precise localization of electrodes (e.g., Herry and Garcia 2002; Bissonette et al. 2008), microdialysis probes (e.g., Van Dort et al. 2009), receptor binding sites and mRNAs expression (e.g., Amargós-Bosch et al. 2004; Lidow et al. 2003), as well as for anatomical guidance of neuroimaging studies (e.g., Barrett et al. 2003) and tracing neural connections to and from mouse frontal cortical areas (Charbonneau et al. 2012; Parent et al. 2010).

With this review, we address a topic which is essential for the understanding of the functions of different mouse PFC subareas, and ultimately for the iConnectome (e.g., Hintiryan et al. 2012) and the digital database for multidisciplinary information incorporation, interpretation and reference system (Hawrylycz et al. 2011).

Acknowledgments This study was supported by Grant RO1 MH61578 (G.Rajkowska (P.I.); H.B.M.U.). We thank Dr. L.J.A. Huisman for his linguistic assistance, and Drs. W.J.A.J. Smeets, G. Rajkowska and M.P. Witter and the reviewers of this journal for their constructive critical comments on a previous version of this manuscript.

Conflict of interest The authors declare that they have no conflict of interest.

Appendix 1: Characteristics

Cytoarchitectonic characteristics of boundaries (Van de Werd et al. 2010).

Medial prefrontal subareas anterior to the corpus callosum

Boundary **Fr1/Fr2** *(frontal areas 1 and 2)*

Columns are seen in both **Fr1** (frontal area 1) and **Fr2** (frontal area 2), but more prominent and more densely packed in **Fr2**. The columns regard the layers V and VI, but in **Fr1** the arrangement of cells in the layer VI might be horizontal instead of columnar.

The size of the cells of the columns is larger in **Fr1** than in **Fr2**.

The layer V rises gradually in **Fr1** to reach its most superficial level at the transition from **Fr1** to **Fr2**. This is due to the progressive loss of cells in the layer IV of **Fr1** as it approaches the agranular **Fr2**.

The layer II shows clefts in **Fr1**, but in **Fr2** the layer II cells join into a smooth, less interrupted layer.

Boundary **Fr2/ACd** *(dorsal anterior cingulate area)*

Columns are seen in both areas in the layers V and VI, but they are more densely packed in **ACd** (dorsal anterior cingulate area) than in **Fr2**.

The size of the cells of the columns is smaller in **ACd** than in **Fr2**.

In the layer II of **Fr2** the most superficial cells show a smooth surface with layer I, in **ACd** the cells of the layer II are very much concentrated on its surface, which is irregular.

Boundary **ACd/PL** *(prelimbic area)*

Columns are visible in **ACd**, not in **PL**. The layer VI in **ACd** is part of the columnar structure seen in the layers V and VI of that area, but in **PL** the cells of the layer V are not arranged in a recognizable structure and the cells of its layer VI are arranged in horizontal lines, parallel to the pial surface.

The layer V shows columns in **ACd**, but not in **PL**. The cells of the layer V in **PL** are, however, densely packed. The cells of layer V are larger in **PL** than in **ACd**.

The cells of the layer III in **ACd** are less densely packed than the cells of the layer III in **PL**. The layer II in **ACd** is narrow, its cells are concentrated on its surface, in **PL** the layer II is broader and its cells are spread more equally over the whole layer.

Anterior to the fornix minor of the corpus callosum the deeper layers of the PFC are not visible and the features of layer II and less so of layer III will then be the decisive factors in positioning the boundary.

Boundary **PLd/PLv** *(the dorsal and ventral part of PL)*

In the prelimbic area (**PL**) we distinguish a dorsal part **PLd** and a ventral part **PLv**.

The layers V and VI are more densely packed in the ventral than in the dorsal part of **PL**. The basic structure of these layers remains, however, the same for the ventral as well as the dorsal part of **PL**.

In both **PLd** and **PLv**, the cells of the layer III are less densely packed than in the neighboring layers. As a result the layer III is lighter in appearance in both parts of **PL**. The layer II is narrower and more densely packed in **PLd** than in **PLv**, where the layer is broader and the cells are less densely packed.

Boundary **PL/MO** *(medial orbital area)*

In the most frontal part of the PFC **PL** borders **MO**, due to absence of the infralimbic area (**IL**) at that level. The main characteristic of the boundary between **PL** and medial orbital area (**MO**) is the equally dispersed cells of the layer II in **MO** in contrast to the unequal spread of cells in the layer II in **PL**.

Layer III separates layer II and V more clearly in **PL** than in **MO**.

Boundary **PL/IL** *(infralimbic area)*

The layers II, III and V are well distinguishable from each other in **PL**, but in the infralimbic area (**IL**) they are homogeneous. Some cells of the layer II of **IL** spread into the layer I, but not in **PL** or much less so. The cells in layers II-V are smaller in IL than in PL.

The contrast between the clearly distinguishable layer III in **PL** and the homogeneity of this layer with the neighboring layers in **IL** is often the easiest sign to determine the boundary between the two areas.

It should be noted that the homogeneity of the layers II, III and V is not always complete in **IL** as sometimes the layer II might be still distinguishable from the other layers. The layer VI shows a horizontal arrangement of its cells in both **PL** and **IL** (infralimbic area).

Boundary **IL/MO**

The boundary between the infralimbic area (**IL**) and the medial orbital area (**MO**) is characterized mainly by the difference in layer II which is homogeneous with the layers III and V and with spreading of cells of the layer II into layer I in **IL**, while in **MO** layer II has a sharp border to the layer III.

The cells of the layer II are very equally dispersed in **MO**, but less so in **IL**. The cells of layer II are smaller in IL than in **MO**.

Boundary **MO/VO** *(ventral orbital area)*

The boundary between the medial orbital (**MO**) and ventral orbital (**VO**) area is determined mainly by layers I-III. Generally the layer II of the medial orbital area (**MO**) is sharply separated from the layers I and III and the cells in it are rather equally dispersed. In the ventral orbital area (**VO**), the cells of layer II tend to spread into the layer I and the cells in this layer are less densely packed than in **MO**. Also some clustering is present in the layer II in **VO**. The layer III in **MO** may show fine columns, the layer III in **VO** usually does not.

Medial subareas caudally to the genu of the corpus callosum

Boundary **ACd/ACv** *(ventral anterior cingulate area)*

Columns are seen in **ACd** but not in **ACv** (ventral anterior cingulate area).

The cells of the layer VI in **ACd** are part of the characteristic columnar structure of that area, but the cells of the layer VI in **ACv** are arranged in horizontal lines.

The cells of the layer V are arranged in columns in **ACd**, but not in **ACv**. The cells of the layer V are densely packed in **ACv**, not in **ACd**.

In both **ACd** and **ACv**, the layer III is easily distinguishable from the neighboring layers by its light appearance.

The layer II of **ACd** is narrow and its cells are irregularly concentrated on its surface while in **ACv** the layer II is broader and the cells are spread more equally.

Boundary **ACvd/ACvv**

In **ACv** a dorsal part (**ACvd**) and a ventral part (**ACvv**) are distinguished.

In all layers, the cells are more densely packed in the ventral than in the dorsal part of **ACv**. In both **ACvd** and **ACvv**, the layer III has a light appearance due to the fact that its cells are less densely packed than in the neighboring layers.

The layer II is narrower and more concentrated in **ACvd** than in the broader layer II of **ACvv**.

Difference between **PL** *and* **ACv**

The contrast of the layer III with the neighboring layers is clearer in **ACv** than in **PL**. As a consequence the difference between the areas **ACd** and **ACv** is less than between the areas **ACd** and **PL**. The border between the layers II and I is sharper in **ACv** than in **PL**.

Ventral PFC subareas

The ventral areas are known as the ventral orbital (**VO**), the ventrolateral orbital (**VLO**) and the lateral orbital (**LO**) area and they are distinguished by the following characteristics.

Boundaries **VO/VLO/LO**

In **VO**, the cells of the layer II are not arranged in a recognizable structure. They are unequally spread with some cells spreading into the layer I seeking contact to the retrobulbar region. Also some clustering is present in the layer II in **VO**.

In **VLO**, the cells of the layers II and III are arranged in curvilinear vertical columns. **VLO** is usually situated at the ventral notch, the indentation seen on the ventral side of the frontal lobe. The main characteristic of the lateral area (**LO**) is the clustering of cells in its layer II with a sharp transition of that layer to the layer III.

The **VLO** differs from its posterior part, **VLOp**, by the following features. In **VLO**, the layers III, V and VI are separated by open zones of low cell density. In the posterior part of **VLO**, distinguished as **VLOp**, however, all layers are more homogeneous.

Lateral PFC subareas

Boundary of the granular (**G**) *or dysgranular insular cortex* (**DI**) *with the dorsal agranular insular area 1* (**AId1**)

In the frontal part of the PFC, the dorsal agranular insular area 1 (**AId1**) borders the granular cortex (**G**), but in the caudal part of the PFC **AId1** borders the dysgranular cortex (**DI**).

Columns are seen very clearly in the layers V and VI in **AId1**, not at all or much less impressive and less closely packed in **G** or **DI**.

The cells of layer V are smaller in **AId1** than in **G** or **DI**.

The layers II, III and IV are homogeneous in **DI**, but in **AId1** the layer IV is absent and the layers II and III are well distinguishable from each other.

The cells of the layer III are less densely packed in **AId1** than in **G** or **DI**.

Boundary **AId1/AId2** *(dorsal agranular insular area 2)*

Columns are seen in both areas, but they are more densely packed in **AId2** than in **AId1**.

The cells of the layer V are smaller in **AId2** than in **AId1**.

The cells of the layer III are less densely packed in **AId2** than in **AId1**.

The layer II is broad in both areas. In **AId1** layer II cells are densely packed, but in **AId2** the layer II is broken by clefts, its cells partake in the columnar structure of the area and some cells spread into the layer I.

Boundary **AId1/AIp** *(posterior agranular insular area)*

In the posterior agranular insular area (**AIp**), the cortical layers and the claustrum are well separated from each other. If the cell-sparse zones between the layers are included as sublayers, 8 or more (sub)layers can be distinguished. In **AId1**, the layers are contingent and a columnar arrangement of the cells of the layers V and VI is visible. The cells of layer V of **AIp** are smaller than the cells of layer V in **AId1**.

Boundary **AId2/LO**

Columns are seen in the layers VI, V and II in **AId2**, but not in **LO**. Layer I is narrow in **LO**, broad in **AId2**. The layer II in **AId2** is broad and cells spread to layer I. In **LO** the layer II shows marked clustering of cells.

Appendix 2

Abbreviations in the Franklin and Paxinos atlas (2008)

AI	Agranular insular cortex
AID	Agranular insular cortex, dorsal part
AIP	Agranular insular cortex, posterior part
AIV	Agranular insular cortex, ventral part
Cg1	Cingulate cortex, area 1
Cg2	Cingulate cortex, area 2
Cl	Claustrum
DI	Dysgranular insular cortex
DLO	Dorsolateral orbital cortyex
DP	Dorsal peduncular cortex
fmi	Forceps minor of the corpus callosum
Fr3	Frontal cortex, area3
FrA	Frontal association cortex
GI	Granular insular cortex
IL	Infralimbic cortex
LO	Lateral orbital cortex
M2	Secondary motor cortex
MO	Medial orbital cortex
PrL	Prelimbic cortex
RSD	Retrosplenial dysgranular cortex
RSG	Retrosplenial granular cortex
VO	Ventral orbital cortex

Abbreviations in the Hof et al. atlas

ACd	Anterior cingulate cortex, dorsal part
ACv	Anterior cingulate cortex, ventral part
AId	Agranular insular cortex, dorsal part
AIp	Agranular insular cortex, posterior part
AIv	Agranular insular cortex, ventral part
CLA	Claustrum
DP	Dorsal peduncular area
fa	Corpus callosum, anterior forceps

FRA	Frontal association area
FRP	Frontal pole
GU	Gustatory cortex
IG	Indusium griseum
IL	Infralimbic area
MOs	Secondary motor cortex
ORBl	Orbital cortex, lateral part
ORBm	Orbital cortex, medial part
ORBvl	Orbital cortex, ventrolateral part
PL	Prelimbic area
rf	Rhinal fissure
TTd	Tenia tecta, dorsal part

Abbreviations in the Rose atlas

ai 1	Area insularis agranularis anterior
ai 2	Area insularis agranularis posterior
i 1	Area insularis granularis anterior
i 2	Area insularis granularis posterior
IRa α	Area infraradiata ventralis anterior
IRb α	Area infraradiata intermedia anterior
IRc α	Area infraradiata dorsalis anterior
IRa β	Area infraradiata ventralis posterior
IRb β	Area infraradiata intermedia posterior
IRc β	Area infraradiata dorsalis posterior
Praecag	Regio praecentralis agranularis
Praecgr	Regio praecentralis granularis

Abbreviations in the Wree et al. study

C1; 2; 3; 4	Area cingularis 1; 2; 3; 4
Cl	Claustrocortex
Prc_m	Area praecentralis medialis

References

Amargós-Bosch M, Bortolozzi A, Puig MV, Serrats J, Adell A, Celada P, Toth M, Mengod G, Artigas F (2004) Co-expression and in vivo interaction of serotonin1A and serotonin2A receptors in pyramidal neurons of prefrontal cortex. Cereb Cortex 14:281–299

Barrett D, Shumake J, Jones D, Gonzales-Lima F (2003) Metabolic mapping of mouse brain activity after extinction of a conditioned emotional response. J Neurosci 23:5740–5749

Bissonette GB, Martins GJ, Franz ThM, Harper ES, Schoenbaum G, Powell EM (2008) Double dissociation of the effects of medial and orbital prefrontal cortical lesions on attentional and affective shifts in mice. J Neurosci 28:11124–11130

Brodmann K (1909) Vergleichende Lokalisationslehre der Grosshirnrinde. Barth Verlag, Leipzig, pp 324

Caviness VS Jr (1975) Architectonic map of neocortex of the normal mouse. J Comp Neurol 164:247–263

Charbonneau V, Laramée ME, Boucher V, Bronchti G, Boire D (2012) Cortical and subcortical projections to primary visual cortex in anophthalmic, enucleated and sighted mice. Eur J Neurosci 36:2949–2963

Dalley JW, Cardinal RN, Robbins TW (2004) Prefrontal executive and cognitive functions in rodents: neural and neurochemical substrates. Neurosci Biobehav Rev 28:771–784

De Vries I (1912) Über die Zytoarchitektonik der groszhirnrinde der Maus und über die Beziehung der einzelnen Zellschichten zum Corpus callosum auf Grund von experimentellen Läsionen. Folia Neuro-Biol 6:289–322

Franklin K, Paxinos G (2008) The mouse brain in stereotaxic coordinates, 3rd edn. Academic Press, Elsevier, San Diego

Groenewegen HJ (1988) Organization of the afferent connections of the mediodorsal thalamic nucleus in the rat, related to the mediodorsal–prefrontal topography. Neuroscience 24:379–431

Groenewegen HJ, Berendse HW, Wolters JG, Lohman AHM (1990) The anatomical relationship of the prefrontal cortex with the striatopallidal system, the thalamus and the amygdala: evidence for a parallel organization. In: Uylings HBM, Van Eden CG, De Bruin JPC, Corner MA, Feenstra MGP (eds) Progress in brain research. In: The prefrontal cortex; its structure, function and pathology, vol 85. Elsevier Science Publishers, Amsterdam, pp 95–118

Groenewegen HJ, Uylings HBM (2010) Organization of prefrontal–striatal connections. In: Steiner H, Tseng KY (eds) Handbook basal ganglia structure and function: a decade of progress. Academic press, San Diego, pp 353–365

Hawrylycz M, Baldock RA, Burger A, Hashikawa T, Johnson GA, Martone M, Ng L, Lau L, Larsen SD, Nissanov J, Puelles L, Ruffins S, Verbeek F, Zaslavsky I, Boline J (2011) Digital atlasing and standardization in the mouse brain. PLoS Comput Biol 7(2):e1001065. doi:10.1371/journal.pcbi.1001065

Heidbreder CA, Groenewegen HJ (2003) The medial prefrontal cortex in the rat: evidence for a dorso-ventral distinction based upon functional and anatomical characteristics. Neurosci Biobehav Rev 27:555–579

Herry C, Garcia R (2002) Prefrontal cortex long-term potentiation, but not long-term depression, is associated with the maintenance of extinction of learned fear in mice. J Neurosci 22:577–583

Hintiryan H, Gou L, Zingg B, Yamashita S, Lyden HM, Song MY, Grewal AK, Zhang X, Toga AW, Dong H-W (2012) Comprehensive connectivity of the mouse main olfactory bulb: analysis and online digital atlas. Front Neuroanat. doi:10.3389/fnana.2012.00030

Hoover WB, Vertes RP (2011) Projections of the medial orbital and ventral orbital cortex in the rat. J Comp Neurol 519:3766–3801

Hof PR, Young WG, Bloom FE, Belichenko PV, Celio MR (2000) Comparitive cytoarchitectonic atlas of the C57BL/6 and 129/Sv mouse brains. Elsevier, Amsterdam

Krieg WJS (1946) Connections of the cerebral cortex. I. The albino rat. A. Topography of the cortical areas. J Comp Neurol 84:221–275

Lidow MS, Koh PO, Arnsten AFT (2003) D1 dopamine receptors in the mouse prefrontal cortex: immunocytochemical and cognitive neuropharmacological analyses. Synapse 47:101–108

Parent MA, Wang L, Su J, Netoff T, Yuan L-L (2010) Identification of the hippocampal input to medial prefrontal cortex in vitro. Cereb Cortex 20:393–403

Paulussen M, Jacobs S, Van Der Gucht E, Hof PR, Arckens L (2011) Cytoarchitecture of the mouse neocortex revealed by the low-molecular-weight neurofilament protein subunit. Brain Struct Funct 216:183–199

Ray JP, Price JL (1992) The organization of the thalamocortical connections of the mediodorsal thalamic nucleus in the rat,

related to the ventral forebrain-prefrontal cortex topography. J Comp Neurol 323:167–197

Reep RL, Corwin JV, King V (1996) Neuronal connections of orbital cortex in rats: topography of cortical and thalamic afferents. Exp Brain Res 111:215–232

Rose M (1929) Cytoarchitektonischer Atlas der Groszhirne der Maus. J Psychol Neurol 40:1–51

Schilman EA, Uylings HBM, Galis-de Graaf Y, Joel D, Groenewegen HJ (2008) The orbital cortex in rats topographically projects to central parts of the caudate-putamen complex. Neurosci Lett 432:40–45

Tsuneda N (1937) Zur Cytoarchitektonik des Neocortex des Mäusegehirns. Okajimas Folia Anat Jpn 15:1–47

Uylings HBM, Van Eden CG (1990) Qualitative and quantitative comparison of the prefrontal cortex in rat and primates, including humans. In: Uylings HBM, Van Eden CG, De Bruin JPC, Corner MA, Feenstra MGP (eds) Progress in brain research. The prefrontal cortex; its structure, function and pathology, vol 85. Elsevier Science Publ., Amsterdam, pp 31–62

Uylings HBM, Sanz–Arigita EJ, De Vos K, Pool CW, Evers P, Rajkowska G (2010) 3-D Cytoarchitectonic parcellation of human orbitofrontal cortex, Correlation with postmortem MRI. Psychiat Res Neuroimag 183:1–20

Van De Werd HJJM, Uylings HBM (2008) The rat orbital and agranular insular prefrontal cortical areas: a cytoarchitectonic and chemoarchitectonic study. Brain Struct Funct 212:387–401

Van De Werd HJJM, Rajkowska G, Evers P, Uylings HBM (2010) Cytoarchitectonic and chemoarchitectonic characterization of the prefrontal cortical areas in the mouse. Brain Struct Funct 214:339–353

Van Dort CJ, Baghdoyan HA, Lydic R (2009) Adenosine A(1) and A(2A) receptors in mouse prefrontal cortex modulate acetylcholine release and behavioral arousal. J Neurosci 29:871–881

Van Eden CG, Uylings HBM (1985) Cytoarchitectonic development of the prefrontal cortex in the rat. J Comp Neurol 241:253–267

Wree A, Zilles K, Schleicher A (1983) A quantitative approach to cytoarchitectonics. VIII. The areal pattern of the cortex of the albino mouse. Anat Embryol 166:333–353